Developmental Biology 456 (2019) 47–62

Contents lists available at ScienceDirect

Developmental Biology

journal homepage: www.elsevier.com/locate/developmentalbiology

Original research article

A novel group of secretory cells regulates development of the immature intestinal stem cell niche through repression of the main signaling pathways driving proliferation

Jianlong Li, Margaret R. Dedloff, Katrina Stevens, Lea Maney, Morgan Prochaska, Cintia F. Hongay, Kenneth N. Wallace *

Department of Biology, Clarkson University, Potsdam, NY, USA

ARTICLE INFO

Keywords:
Zebrafish
Intestine
Stem cell regulation
Secretory cell
Wnt
EGF
IGF
Proliferation

ABSTRACT

The intestinal epithelium has constant turnover throughout the life of the organ, with apoptosis of cells at the tips of folds or villi releasing cells into the lumen. Due to constant turnover, epithelial cells need to be constantly replaced. Epithelial cells are supplied by stem cell niches that form at the base of the interfold space (zebrafish) and crypts (birds and mammals). Within the adult stem cell niche of mammals, secretory cells such as Paneth and goblet cells play a role in modulation of proliferation and stem cell activity, producing asymmetric divisions. Progeny of asymmetric divisions move up the fold or villi, giving rise to all of the epithelial cell types. Although much is known about function and organization of the adult intestinal stem cell niche, less is understood about regulation within the immature stem cell compartment. Following smooth muscle formation, the intestinal epithelium folds and proliferation becomes restricted to the interfold base. Symmetric divisions continue in the developing interfold niche until stem cell progeny begin asymmetric divisions, producing progeny that migrate up the developing folds. Proliferative progeny from the developing stem cell niche begin migrating out of the niche during the third week post-embryogenesis (zebrafish) or during the postnatal period (mammals). Regulation and organization of epithelial proliferation in the immature stem cell niche may be regulated by signals comparable to the adult niche. Here we identify a novel subset of secretory cells associated with the developing stem cell niche that receive Notch signaling (referred to as NRSCs). Inhibition of the embryonic NRSCs between 74 hpf to 120 hpf increases epithelial proliferation as well as EGF and IGF signaling. Inhibition of post-embryonic NRSCs (6 hpf to 12 dpf) also increases epithelial proliferation and expression level of Wnt target genes. We conclude that NRSCs play a role in modulation of epithelial proliferation through repression of signaling pathways that drive proliferation during both embryogenesis and the post embryonic period.

1. Introduction

The intestinal stem cell compartment replaces epithelial cells throughout the life of the organ. Intestinal epithelial stem cells reside within the crypt of the mammalian intestine and at the interfold base in zebrafish (Barker, 2014; Crosnier et al., 2005; Wallace et al., 2005b). During the life of the intestine, stem cell progeny migrate out of the crypt or interfold base, differentiate into either enterocytes or secretory cells, migrate up the villi or fold, undergo apoptosis at the tips and are extruded into the intestinal lumen (Barker, 2014; Crosnier et al., 2005; Wallace et al., 2005b).

Within the adult mammalian crypt, stem cell proliferation is positively regulated by Wnt, Notch, and Epidermal Growth Factor (EGF) signaling pathways that originate from both the interdigitated secretory cells (Paneth cells in small intestine and goblet cells in large intestine) and the underlying mesenchyme (Barker, 2014). While Wnt and EGF signaling drive proliferation, these pathways are also negatively regulated to prevent over production of stem cells and their progeny. Wnt signaling is negatively regulated by *RNF43* (Koo et al., 2012) and *ZNRF3* (Hao et al., 2012) E3 ubiquitin ligases, which target Frizzled and Lrp6 Wnt receptors for ubiquitin-mediated endocytosis and lysosomal degradation. In contrast, R-spondins, in combination with Lgr4, bind RNF43 and ZNRF3 to target their removal from the membrane. Removal of RNF43 and ZNRF3 allow Wnt receptors to remain at the cell surface,

* Corresponding author.
E-mail address: kwallace@clarkson.edu (K.N. Wallace).

https://doi.org/10.1016/j.ydbio.2019.08.005
Received 27 February 2019; Received in revised form 23 July 2019; Accepted 5 August 2019
Available online 6 August 2019

resulting in increased signaling (Hao et al., 2012; Xie et al., 2013). EGF signaling is negatively regulated by Lrig1, which inhibits ErbB activity (Wong et al., 2012). Absence of Lrig1 results in enlarged stem cell niches (Wong et al., 2012).

Insulin-like Growth Factor (IGF) signaling within the intestine promotes epithelial and mesenchymal proliferation as well an increased prevention of apoptosis (Kuemmerle, 2012). Many components of IGF signaling are expressed within subepithelial myofibroblasts and lamina propria while IGF receptors are expressed in enterocytes, targeted to basolateral membranes (Shoubridge et al., 2001; Winesett et al., 1995). IGF ligand activity is also positively and negatively regulated by six secreted Insulin-like Growth Factor Binding Proteins (IGFBPs). IGFBPs bind to IGF ligands to alter interaction with IGF receptors (Firth and Baxter, 2002; Kuemmerle, 2012). IGFBPs can function to sequester IGF ligand while others can facilitate receptor binding (Firth and Baxter, 2002). Many of the pathways driving epithelial stem cell proliferation are modified by additional factors that appear to regulate both upper and lower limits of proliferation. These modifications allow for fine tuning of the number of stem cells within the adult crypt.

While signaling pathways can be fine tuned from within the crypt, tuft cells may play a role in regulating proliferation of stem cells from a distance. Tuft cells are a novel differentiated epithelial cell type that does not undergo additional proliferation following differentiation (Westphalen et al., 2014). Tuft cells have some enteroendocrine secretory properties (Bjerknes et al., 2012). Tuft cells develop chemoreception, as they have aspects of taste receptors (Sato, 2007). Tuft cells do not arise from the secretory lineage that gives rise to enteroendocrine and goblet cells (Bjerknes et al., 2012; Westphalen et al., 2014). Tuft cells are closely associated with enteric ganglia (Bezencon et al., 2008; Hayakawa et al., 2017; Schutz et al., 2015). Tuft cells play a role in signal transduction, as ablation of tuft cells inhibits stimulatory roles of neurons in growth of epithelial colonic organoids (Westphalen et al., 2014). Vagotomy in the stomach results in down regulation of Wnt and Notch signaling in $Lgr5^{+}$ stem cells and reduced tuft cells (Zhao et al., 2014). Interaction of tuft cells and enteric neurons suggests a mechanism for interaction between crypts and coordination of stem cell proliferation throughout the intestinal epithelium.

Prior to yolk exhaustion at the end of zebrafish embryogenesis, the intestine must be able to absorb nutrients and act as a barrier to the external environment. As a result, zebrafish need to develop some characteristics of the mature intestine at an earlier relative time than species with a larger yolk (birds) or internal development (placental mammals). Two of the mature characteristics zebrafish develop are proliferation restricted to the fold base and functional smooth muscle for peristalsis. Mechanisms that drive these developmental events are likely to be shared between zebrafish, birds and mammals. They are likely to be utilized at a later relative time in birds and placental mammals.

Initially in the developing embryonic vertebrate intestine, proliferation occurs throughout the epithelium (Shyer et al., 2015; Wallace et al., 2005b). Epithelial proliferation eventually becomes restricted to the base of the developing villi due to the physical folding of the epithelium in mammals and birds. Development of circular and longitudinal smooth muscle surrounding the intestine initiates folding of the intestinal epithelium (Shyer et al., 2013). Folding of the intestinal epithelium creates a local increase in BMP signaling along the villi to inhibit proliferation while lower BMP concentrations remain at the villi base where proliferation continues as the adult stem cell compartment develops (Shyer et al., 2015). In zebrafish, restriction of intestinal epithelial proliferation to the fold base by the end of embryogenesis (5 dpf) (Wallace et al., 2005b) coincides with maturation of the intestinal smooth muscle (Olden et al., 2008). This correlation suggests that zebrafish smooth muscle maturation may also promote epithelial folding and restriction of proliferation to the fold base.

While much is known about the cells and signaling involved in regulation of the adult stem cell compartment, less is known about cell types and signaling involved in the developmental steps between proliferation restriction to the base of the developing folds or intervilli to development of the adult stem cell niche. Restriction of proliferation to the interfold base occurs at 5 dpf in zebrafish (Wallace and Pack, 2003). Proliferation restriction occurs in the intervilli space at e16.5 in mice (Korinek et al., 1998). Formation of adult stem cell niche occurs by 33 dpf in zebrafish (Crosnier et al., 2005) and p15 in mice (Yanai et al., 2017). While the developing stem cell niche depends on a set of signals to positively regulate proliferation, there is also likely to be signals that down regulate epithelial proliferation. The combination of positive and negative proliferative signals would then fine tune the number of immature stem cells as the compartment develops.

Here we identify cells interspersed at the interfold intestinal base within developing stem cell compartments. These cells are identified by reception of Notch signaling as well as the pan-secretory cell marker, 2F11 (and thus referred to as Notch receiving secretory cells-NRSCs). One group of NRSCs form during the end of embryogenesis (74 hpf to 120 hpf and referred to as eNRSCs) and a second group forms during the first week post embryogenesis (6 dpf to 12 dpf and referred to as pNRSCs). We find that NRSCs down regulate epithelial proliferation both during the end of embryogenesis and during the first week post embryogenesis. Interruption of both e and pNRSC development results in moderate proliferation increases, suggesting these cells fine tune the upper end of proliferative activity. eNRSCs act through downregulation of the EGF and IGF pathways during the end of embryogenesis. pNRSCs act through downregulation of Wnt signaling during the first week post embryogenesis. eNRSCs may also have an additional role in maintaining proliferative levels in the post embryonic period (6 dpf to 12 dpf).

2. Materials and methods

2.1. Fish stocks

Fish maintenance and matings were performed as previously described (Westerfield, 1993). AB wild type fish were used for procedures without transgenic lines (Westerfield, 1993).

2.2. Detection of notch receiving cells (NRSCs)

To detect Notch receiving secretory cells (NRSCs), the transgene *Tg(T2KTp1glob:creER^{T2})^{jh12}* (hereinafter referred to as NCre driver) was used to drive expression of inducible CreER^{T2} in cells that receive Notch signaling (Wang et al., 2011). The transgene drives CreER^{T2} from 12 RBP-Jκ-binding sites and a minimal β-globin promoter. The Ncre driver is combined with the transgene *Tg(T2Kβactin:loxP-stop-loxP-hmgb1-mCherry)^{jh15}* (hereinafter referred to as *Cre* responder) to mark NRSCs with nuclear mCherry expression (Wang et al., 2011). Induction of CreER^{T2} with 4-Hydroxytamoxifen (4OHT, T176, Sigma) for a 2-h period was performed at the same concentration (5 μM) as previously reported, diluted from a stock concentration of 10 mM dissolved in 100% ethanol (Wang et al., 2011). Following induction, NRSCs and their progeny continuously express nuclear mCherry.

2.3. Analysis of NRSCs

To determine co-expression with secretory cell specific transcription factors, the transgene *Tg[nkx2.2a:mEGFP]* (Ng et al., 2005) was individually crossed into the Ncre driver/Cre responder combination (Wang et al., 2011). The null mutation *ascl1a ^{t25215}* (Pogoda et al., 2006) was used in analysis of NRSCs.

2.4. Inhibition of Wnt, EGF and IGF signaling

To inhibit the endpoint of the Wnt signaling pathway, ectopic expression of the dominant negative TCF from the transgenic Tg (HS:TCFΔC)^{W74} (Martin and Kimelman, 2012) was induced by increasing temperature to 37 °C for 20 min, followed by return to 28.5 °C embryo

media (embryos) or system water (one week post-embryonic fish). WT controls were heat shocked for the same period in as the DN TCF.

EGF signaling was inhibited for 2 h periods with the cell-permeable EGF kinase inhibitor AG-1478 (Cayman Chemical 10010244) at the previously reported concentration of 3 μM solubilized in DMSO (Budi et al., 2008). Control embryos were exposed to an equal concentration of DMSO for the same 2-h periods. Relative expression of myelin basic protein between control and AG-1478 inhibited embryos was compared for internal control to demonstrate activity of EGF inhibition.

IGF signaling was inhibited for 2 h periods with NVP-AEW541 (Cayman Chemical 13641) at the previously reported concentration of 5 mM solubilized in DMSO (Chablais and Jazwinska, 2010). Control embryos were exposed to an equal concentration of DMSO for the same 2-h periods. Intensity of phosphorylated IGF 1 receptor was compared between control and NVP-AEW541 inhibited embryos for an internal control to demonstrate activity of IGF inhibition.

2.5. DAPT exposure

Embryos or larvae were exposed to either DAPT (0.05 mM) or an equivalent concentration of DMSO as a control. 5dpf embryos were treated with 0.05 mM of DAPT or DMSO from 74 hpf to 120 hpf, and intestines were isolated at 120 hpf. DAPT or DMSO exposure during the first week of the post embryonic phase were done in three alternating days (6 dpf, 8 dpf, 10 dpf) with the same concentrations of DAPT or DMSO for 2 h per day. Intestines were isolated at 11 dpf.

2.6. EdU and BrdU incorporation

Embryos and larvae are injected with a microcapillary needle in the intestinal region (either directly into the intestine or peritoneal space) with either 2.5 mM 5-ethynyl-2′-deoxyuridine (EdU) or 50 mM 5-Bromo-2′-deoxyuridine (BrdU). EdU or BrdU injected individuals were grown to indicated time. At end of the period, each group was fixed in 4% formaldehyde, 2 h to overnight. Incorporation of EdU was detected following the standard protocol for the 488 Click-it Kit imaging kit (Invitrogen). For detection of BrdU, individuals were exposed to 0.2 N HCL for 30 min at room temperature followed by anti- BrdU antibody (Sigma) incubation overnight at 4 °C. Secondary antibody is Alexa Fluor 594-conjugated anti mouse IgG (1:500) (Molecular Probes-Invitrogen). Previously, control single labeling of EdU or BrdU was processed for detection of the opposite nucleotide (injected at 4 dpf and grown to 5 dpf) (Li et al., 2019). While the injected nucleotide was detected, there was no cross-reactivity for the opposite nucleotide demonstrating the specificity of EdU and BrdU detection.

2.7. Imaging and histology

Samples imaged in whole mount were dissected using #5 Dumont Tweezers from the specimen and intestines were mounted on a slide in Vectashield (Vector Laboratories). Samples are processed for histology by infiltration and embedded in glycol methacrylate (JB4 plus; Poly-Sciences). Sections were cut on a Leica RM2135 microtome.

2.8. RNA isolation, reverse-transcription and qPCR

Intestines were dissected for whole mount from 5 dpf embryos or 11 dpf post-embryonic fish using Dumont #5 forceps. Total RNA was isolated using Trizol reagent (Invitrogen) according to manufacturer's instructions. RNA was treated with DNase I (Qiagen) and purified by RNeasy Mini kit (Qiagen). RNA gel electrophoresis was performed to confirm integrity. cDNA was reverse-transcribed by SuperScript II First-Strand synthesis kit (Invitrogen). Quantitative PCR (qPCR) was performed using Fast EvaGreen qPCR 2X Master Mix (Biotium) SYBR reagent, appropriate primers (see below), and reaction mixtures along with their corresponding minus RT controls were aliquoted onto 96-well plates covered with MicroAmp™ Optical Adhesive Film (ThermoFisher Scientific). The qPCR reactions were performed in a CFX96 Touch Real-time PCR Detection System (Bio-Rad). The amplification program used was as follows: 95 °C for 3 min followed by 40 cycles: 60 °C for 45 s and 95 °C for 15 s, followed by melt curve analysis. The housekeeping gene, β-actin 1 is used to normalize relative gene expression. Minus RT controls were used to subtract amplification due to remaining genomic DNA in samples. After removing amplification signals from minus RT controls, relative gene expression was normalized to β-actin1 and calculated by ΔΔ Ct method. Standard deviation was calculated between biological replicates for control (DMSO treated) and experimental (DAPT or inhibitor treated). Statistical analyses (Student's T-Test) were done with GraphPad Prism 6. Each experiment was done in triplicate (three biological replicates and as well as three technical replicates of each sample).

The primer sequences used were as follows (5′ to 3'): *beta-actin* 1 F: CGAGCAGGAGATGGGAACC, R: CAACGGAAACGCTCATTGC (McCurley and Callard, 2008); *ascl1b* F: GCGGCGAACAAGAAGATGAG, R: GCGTTGGAGACGGATGGAG (Wang et al., 2014); *axin2* F: GCGACACAGCGGGTACAGT, R: ACTCCGGCTGCTGCGAATGT; *cdx1a* F: GGCATGCACTGCTTAAAACATATG, R: TCAGAACTCGGAGGATTATTTT (Cheesman et al., 2011); *cyclinD1* F: AGGCTTTTGAAACGTAAGCCTGCGG, R: AGGTACACTTGGGCATCCGTGCA; *myca* F: CCAGCAGCAGTGGCAGCGAT, R: GGGGACTGGGGTACCTCGACTC (Neal et al., 2013); *NT1* (*neurotensin 1*) F: AAAGCCTCCCGCAAACAGA, R: CACCGGGTGAAGTTTGATGTAG (Cheesman et al., 2011); *sox9b* F: ATACAGAGTACAGCGAGCAGCACA, R: GCGCAAGTATGTGTGTGTGTGTGT (Sun et al., 2013).

egfra F: GAACAAGGCGTAAAAGAGTTGC, R: GTCCCCACGTTACATAAATGGT; *egf* F: TCTTACTTCTGCACCTGTCCTG, R: ATGATCACAATCCACAGCTTTC; *btc* F: CCCAGCGAATAGGACTGTGT, R: TTTGGAC AGGCAGAGAAGTGT; *hbegfa* F: GA TGATGATGTTGAAGAAGACGAG, R: ACTTGGGTCTTTGGGTTGACT; *hbegfb* F: ATTTCTGCATTCATGGAGTGTG, R: GCAGGGTGAATACGTGACATCT; *igf1a*: F: GGGCA TTGGTGTGA TGTCTT, R: CCAGTGAGAGGGTGTGGGTA; *igf1b*: F: CCAAAATCCTTAATGAGTAACTTAGCA, R: AGACATTTTCAACAGGAAA CAGC; *igf2a*: F: TGAAGTCGGAGCGAGATGTT, R: GGAGTACTTCACATTTATGGTGTCC; *igf2b*: F: AGCTGGTGGACGCTCTACA, R: GAGAAC GTCGACTGTTTGACC; *igf1r*: F: GCAACCTGCAAATCAACATC, R: CTGGATCAGCCCCATGAA (Schall et al., 2015).

2.9. Statistical analysis

Determination of significant differences between control and experimental samples was identified using Student's *t*-test. Results with P values of <0.05 were considered statistically significant. Statistically significant values are indicated by asterisks in the bar graphs. The number of asterisks indicate increasing significant differences with lower P values indicated in the respective legend. In experiments with multiple groups, we performed a one-way analysis of variance (ANOVA) to determine whether there were differences in the averages between the groups.

Differences in intensity of IGFr1 phosphorylation between control and experimental samples were calculated by drawing a square region of the same size in confocal images obtained at the same settings. Intensity was calculated in Image J using the integrated density function.

3. Results

3.1. Unique embryonic and post-embryonic Notch receiving secretory cells reside among proliferating cells at the interfold base

Secretory cells have previously been found to develop among proliferating cells at the interfold base within the intestinal epithelium (Li et al., 2019). We hypothesize that these secretory cells play roles in promoting or inhibiting proliferation. Positive and negative regulation may be accomplished by different types of secretory cells residing among proliferating cells at the interfold base. Thus, our experimental approach

was aimed at determining whether there are unique interfold base secretory cells specialized for generating antagonistic proliferative signals. Here we identify two unique groups of secretory cells that receive Notch signaling. The first develops at the end of embryogenesis (74 hpf to 120 hpf), while the second develops during the first week post embryogenesis (6 dpf to 12 dpf).

The secretory cell lineage is specified before 74 hpf with *ascl1a* expression in future secretory cells (Flasse et al., 2013; Roach et al., 2013). *ascl1a* initiates Notch signaling in neighboring cells to drive them into the enterocyte fate (Flasse et al., 2013; Roach et al., 2013). Disruption of Notch signaling increases the number of secretory cells (Flasse et al., 2013; Roach et al., 2013; Troll et al., 2018). Following secretory cell specification, differentiated markers are first observed after 74 hpf (Wallace et al., 2005b). As secretory cells begin differentiating after 74 hpf, we looked for unique interfold secretory cells, using a previously characterized Notch responsive driver and Cre-responder transgene to label and fate map Notch receiving cells.

The Notch responsive Tp1 Cre ER^{T2} produces a Cre inducible with 4OHT (Wang et al., 2011). The transgene *Tg(T2KTp1glob:creER^{T2})^{jh12}* (hereinafter referred to as Ncre driver) was used to drive expression of inducible $CreER^{T2}$ in cells that receive Notch signaling (Wang et al., 2011). The transgene drives $CreER^{T2}$ from 12 RBP-Jκ-binding sites and a minimal β-globin promoter. The Ncre driver is combined with the transgene *Tg(T2Kβactin:loxP-stop-loxP-hmgb1-mCherry)^{jh15}* (hereinafter referred to as *Cre* responder) to mark Notch receiving cells with nuclear mCherry expression (Wang et al., 2011).

The Ncre transgene combination was induced with 4OHT between 74 hpf to 120 hpf (Fig. 1A and B) or 6 dpf to 12 dpf (Fig. 1C and D). Induction during either period identifies isolated cells distributed evenly throughout the intestinal epithelium. Notch receiving cells co-localize with the pan-secretory cell marker 2F11, identifying Notch receiving cells as secretory. In addition, mCherry and pan-secretory 2F11 labeled cells are absent in *ascl1a* mutants, which lack all secretory cells, further suggesting that all of the mCherry labeled cells are secretory cells. Identified cells are referred to as either embryonic Notch receiving secretory cells (eNRSCs) formed between 74 hpf to 120 hpf or post embryonic Notch receiving secretory cells (pNRSCs) formed between 6 dpf to 12 dpf.

Due to the position of e and pNRSCs at the fold base, we hypothesized that they associate with proliferating cells. To identify the position of e and pNRSCs, we induced the Ncre transgene and co-labeled cells in S phase with the nucleotide analog 5-ethynyl-2′-deoxyuridine (EdU). Embryonic NRSCs (eNRSCs) were identified with 4OHT induction at 74 hpf followed by EdU incorporation at 96 hpf. eNRSCs reside within clusters of proliferating cells throughout the intestine at 120 hpf (Fig. 1A) with an average of 149 eNRSCs (± 40; n=10) per intestine. pNRSCs are identified with 4OHT induction and EdU incorporation on three different days between 6 dpf to 12 dpf. pNRSCs are observed interspersed within groups of proliferating cells at 12 dpf (Fig. 1C). pNRSCs are distributed throughout the intestine with an average of 148.6 (± 41.2; n=10). Histological cross section at both 120 hpf (eNRSCs) and 12 dpf (pNRSCs) demonstrate that all NRSCs reside at the interfold base. Both e and pNRSCs are positioned at the edge of the proliferating epithelial cells at the interfold base (120 hpf-Figure 1B and 12 dpf-Fig. 1D).

The Notch responsive Cre driver and the β actin promoter in the Cre responder may not express in all cells that receive Notch signaling. There may be additional Notch receiving secretory cells, or even cells that are not secretory unlabeled by this transgene combination. However these results are similar to the distribution and pattern of cells observed within the intestine using a different Notch responsive mCherry expressing transgene (*Tg(EPV.Tp1-Ocu.Hbb2:hmgb1-mCherry)*) (Lickwar et al., 2017). mCherry reporter expression from the Tp1 Cre ER^{T2}/β actin:loxP-stop-loxP-hmgb1-mCherry combination is consistent with NRSCs being a subset of intestinal epithelial secretory cells.

3.2. NRSCs have characteristics of enteroendocrine cells

Both e and pNRSCs are secretory cells as shown by co-expression of the pan-secretory cell marker, 2F11. However, the pan-secretory cell marker 2F11 identifies all secretory cell types, including goblet cells. Within the mammalian intestine, there are more than 16 different types of enteroendocrine cells (Noah et al., 2011). In zebrafish, all secretory cells arise from a common *ascl1a* expressing precursor but then diverge into a number of different lineages (Flasse et al., 2013; Roach et al., 2013). Mammals utilize a number of different transcription factors to specify enteroendocrine lineages after they diverge from a common progenitor as mutations in these transcription factors result in reductions of specific groups of secretory cells, rather than loss of all enteroendocrine cells (Noah et al., 2011).

To determine whether NRSCs are enteroendocrine, we identified

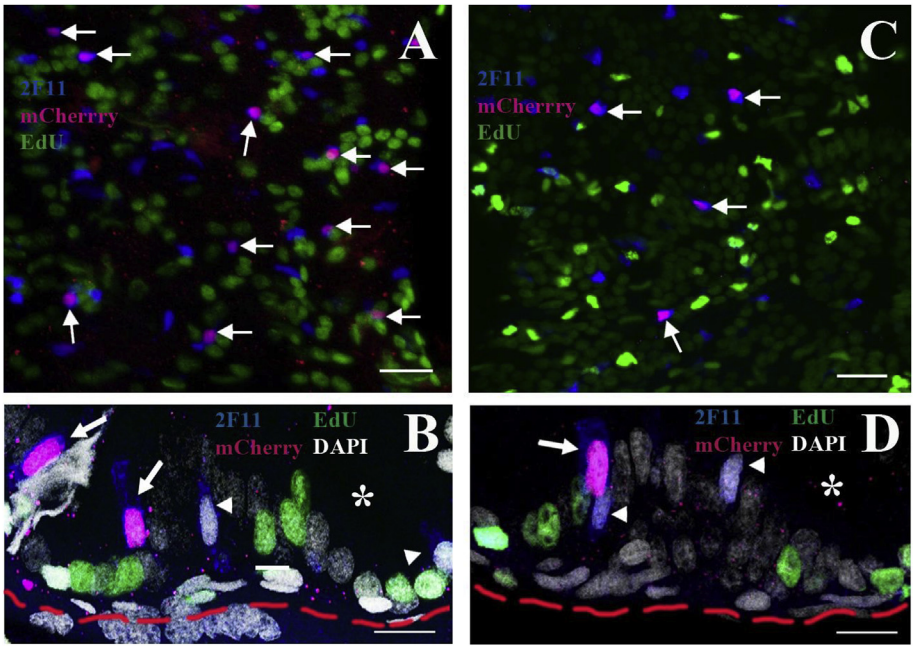

Fig. 1. Notch receiving secretory cells (NRSCs) reside within groups of proliferating cells at the interfold base. A. Whole mount on the fifth day of embryogenesis, some secretory cells (blue) are NRSCS (blue/magenta, arrows) present within groups of proliferating epithelial cells (green). Anterior is to the left. B. In transverse cross-section, NRSCs(blue/magenta) localize on the upper limit of the interfold base (arrows) as judged by their position at the edge of groups of proliferating cells (green). Other secretory cells are also present (blue, arrowheads). C. At the end of the first week post-embryogenesis (12 dpf), NRSCs also reside within proliferating clusters. Not all secretory cells are NRSCs (blue, arrowheads). D. Transverse cross-section as in B. At the end of the first week post-embryogenesis, NRSCs are at the edge of the interfold base (arrow) along with other secretory cells (blue, arrowhead). Green- EdU incorporated cells; Red-nuclear mCherry responder to Tp1 Cre ER^{T2} driver; Blue- 2F11 pan-secretory cell; Grey- DAPI; red dashed line-limit of intestine; asterisk-lumen of intestine; scale bar 10 μM.

whether they co-express *nkx2.2a*. *nkx2.2a* is a transcription factor utilized in a number of enteroendocrine lineages as they begin terminal differentiation (Desai et al., 2008). To visualize expression of *nkx2.2a*, we used the GFP reporter *Tg[nkx2.2a:mEGFP]*. Cells with mCherry and 2F11 have low expression of *nkx2.2a* (Fig. 2A and B- 5 dpf; 2C and E- 12 dpf), suggesting that these are enteroendocrine cells. Low GFP expression in mCherry and 2F11 expressing cells may be due to overlap of the 594 nm conjugated secondary (used for detection of mCherry) into the channel used to image the 488 nm conjugated secondary (for detection of GFP). To determine whether the observed *nkx2.2a*-GFP expression was an artifact due to overlap of fluorescence of the 594 nm secondary into the 488 nm channel, we performed immunohistochemistry utilizing a secondary antibody recognizing the rabbit mCherry antibody that is further separated in emission wavelength from the 488 nm channel. We find a similar pattern of co-localization between GFP and mCherry expressing cells using 488 nm and 633 nm conjugated secondaries (Supplemental Fig. S1).

Low levels of GFP coexpressed with NRSCs may be due to the stage of enteroendocrine cell differentiation. Occasionally we observe cells with high *nkx2.2a*-GFP expression co-localized with 2F11. Many 2F11 positive cells, however, express no or low levels of *nkx2.2a* promoter driven GFP (Fig. 2A and C). Differential *nkx2.2a* by enteroendocirne cells within the zebrafish intestinal epithelium may be similar to the mammalian situation. In mammals, NKX2.2 is expressed in recently differentiated adult 5HT, GLP-1, Gastrin/CCK, and somatostatin enteroendocrine cells before they leave the crypt, but expression is turned off as the cells move onto the villus (Wang et al., 2009). Cells expressing 2F11 with high levels of *nkx2.2a* may be newly differentiated secretory cells. The absence of *nkx2.2a* expression in 2F11 expressing cells may be indicative of more mature enteroendocrine cells.

Within the immature intestinal epithelium, *nkx2.2a* expression may be retained for longer or shorter times following differentiation of enteroendocrine lineages. We suggest that as with mammalian enteroendocrine cells, NRSC expresses *nkx2.2a* as cells differentiate but downregulate *nkx2.2a* as the enteroendocrine cells mature. NRSCs may retain *nkx2.2a* expression longer than other enteroendocrine lineages. The coexpressed GFP may be residual protein that has not yet been degraded within recently differentiated NRSCs. If GFP expression is residual in many NRSCs, it may explain why the GFP appears to be nuclear. NRSCs and enteroendocrine cells in general have a cytoplasm that does not extend far from the circumference of the nuclei (Fig. 1). Therefore, if GFP expression is reduced, the bulk of expression will only occupy a thin margin around the nucleus. The cellular projections are thin and residual GFP expression within these portions of the cell will become faint and hard to detect above background levels.

3.3. NRSCs do not increase in number after formation

We suggest that Notch signaling is one of the final steps in differentiation of the NRSCs. As a result, following Notch signaling, NRSCs are differentiated and no longer proliferate. To confirm that NRSCs no longer increase in number following differentiation, NRSCs were induced with 4OHT and split into two groups. mCherry cells from the first group were recorded soon after 4OHT induction while the second was grown to a later developmental time point to determine whether mCherry cells increase in number. We induced individuals either during embryogenesis or during the post embryonic period. The embryonic 4OHT induction was performed at 74 hpf and fixed at 5 dpf while the second group was grown to 12 dpf. The initial count of mCherry positive cells at 5 dpf produced an average of 136.17 (±31.1, n=12). The second group grown to 12 dpf produced an average count of 148.5 (±45.5, n=12) mCherry positive cells. The post embryonic 4OHT induction was performed at 7 dpf and the first group was fixed at 8 dpf. The count at 8 dpf produced an average of 64.5 (±19.1, n=16) mCherry positive cells. The second group grown to 12 dpf produced an average count of 66.5 (±25.5, n=22) positive mCherry cells. Comparison between the initial and later developmental time points for both the embryonic and post embryonic experiments demonstrate no statistical differences between the two counts using the Student's *t*-test with p values of 0.49 for the embryonic experiment and 0.79 for the post embryonic experiment. While some

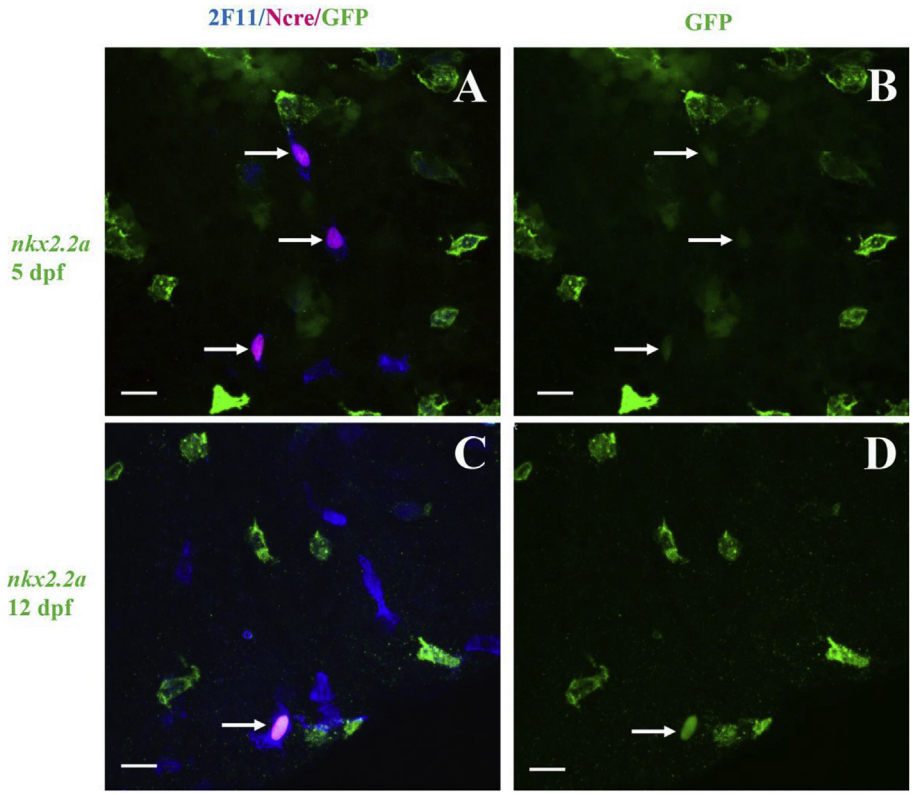

Fig. 2. Notch receiving secretory cells (NRSCs) co-localize with *nkx2.2a*. A group of 2F11 secretory cells (blue) co-label with NRSCs (Ncre-red) and GFP-driven by *nkx2.2a* (A and B- 5 dpf; C and D- 12 dpf). As shown in the GFP only panels, NRSCs have varying levels of *nkx2.2a* (B- 5 dpf and D- 12 dpf). Red-nuclear mCherry responder to Tp1 Cre ER^{T2} driver; Blue- 2F11 pan-secretory cell; Green- GFP driven in specified pattern (*nkx2.2a*). Arrows point to NRSCs in each all panels. Scale bar 10 μm.

NRSCs may undergo additional proliferation or apoptosis, the numbers are consistent with the idea that once formed, the majority of NRSCs are differentiated cells. As NRSCs differentiate, they are likely to remain in the epithelium throughout intestinal development.

3.4. Disruption of Notch signaling between 74 hpf to 11 dpf does not alter secretory cell numbers

We hypothesize that NRSCs receive Notch signaling as a later step in differentiation. Disruption of Notch signaling should interrupt formation of NRSCs to reveal a function for cells in this secretory lineage. However, Notch is used at least twice during early embryogenesis. Earlier Notch signaling involves specification of secretory cells from enterocytes (before 74 hpf) (Roach et al., 2013). After secretory cell specification, individual lineages begin differentiation (Wallace et al., 2005a) and disruption of Notch signaling during the second half of embryogenesis should no longer change numbers of secretory cells. Disruption of Notch signaling after 74 hpf, therefore, should only interrupt NRSC development.

To confirm that disruption of Notch signaling does not alter numbers of secretory cells between 74 hpf to 11 dpf, we disrupted Notch signaling by inhibiting cleavage of the Notch intracellular domain (ICD) using the gamma secretase inhibitor N-[N-(3,5-Difluorophenacetyl)-L-alanyl]-S-phenylglycine t-butyl ester (DAPT). Individuals were exposed to DAPT or DMSO as controls for 2 h followed by wash out into E3 for embryos, or system water for post embryonic fish. Embryonic fish were exposed to DAPT or DMSO each day beginning at 74 hpf to the end of embryogenesis (120 hpf). Post embryonic fish were exposed to DAPT or DMSO on three separate days (6 dpf, 8dpf and 10 dpf).

Following Notch disruption, we compared overall secretory cell numbers using the pan-secretory cell marker 2F11, counting both anterior and posterior regions (regions counted diagrammed in Fig. 3A). We observe no significant changes in overall secretory cell number either during embryogenesis (recorded at 120 hpf- Anterior average DMSO 72.5; DAPT68.2; p value 0.33: Posterior average DMSO 40.6; DAPT 41.4; p value 0.89) or the first week post embryogenesis (recorded at 11 dpf- Anterior average DMSO 89.7; DAPT 91.6; p value 0.83: Posterior average DMSO 61.9; DAPT 54.3; p value 0.29) using the Student's *t*-test. All p values are greater than 0.05 suggesting that application of DAPT after 74 hpf disrupts NRSC development and does not alter secretory cell numbers.

3.5. Interruption of Notch signaling results in increased epithelial cell proliferation during embryonic and post embryonic periods

NRSCs are positioned at the interfold base among proliferating epithelial cells. The location of NRSCs provides them with the opportunity to play a role in regulation of proliferation. If NRSCs regulate epithelial proliferation, then disruption of their development with DAPT should alter the number of cells in S phase.

As mentioned before, we suggest that Notch signaling plays a role in differentiation of NRSCs. Developmental timing of the formation of eNRSCs and pNRSCs suggest that they may play different roles in regulation of proliferation even though they are mixed throughout the intestinal epithelium during the first week post embryogenesis (6 dpf to 12 dpf). We therefore disrupted eNRSCs (74 hpf to 120 hpf), pNRSCs (6 dpf to 11 dpf), or both. Disruption of NRSCs in these three combinations should reveal whether there are different roles for e and pNRSCs. These experiments will determine whether e and pNRSCs interact or support each other in regulation of epithelial proliferation during the first week post embryogenesis.

During NRSC disruption with DAPT, we used the following time course of EdU labeling to capture an appropriate sample of S phase cells. During the second half of embryogenesis (74 hpf to 120 hpf), epithelial proliferation begins to slow as it becomes restricted to the fold base (Wallace et al., 2005a). To evaluate the affect of NRSC loss during the embryonic period we incorporated EdU at 96 hpf and fixed individuals at 120 hpf.

To evaluate the effect of NRSC loss during the post embryonic period, we captured a representative group of proliferating epithelial cells by EdU incorporation on three different days and fixed individuals at 11 dpf. EdU was incorporated on three separate days during the first week post embryogenesis due to the nature of epithelial proliferation during this period. Proliferating epithelial cells during the first week post embryogenesis proceed through one or two rounds of mitosis and then become quiescent (Li et al., 2019). Multiple rounds of proliferating epithelial cells then repeat this process throughout the week. Proliferation rates also vary during the week (Li et al., 2019). Disruption of NRSCs may alter proliferation rates at one point during the week but not others. Sampling on three separate days throughout the week should capture changes in proliferation that occur during the period. Counts of EdU positive cells were taken in both the anterior as well as the posterior region of the intestine (regions counted are diagrammed in Fig. 3A). Previous investigation found that proliferation is primarily located in the intestinal epithelium between 74 hpf to 12 dpf (Li et al., 2019).

eNRSCs were disrupted with DAPT between 74 hpf and 120 hpf and labeled with EdU at 96 hpf. Embryos were fixed at 120 hpf and S phase cells were compared to proliferation of DMSO controls (experimental timeline Fig. 3A). Disruption of eNRSCs between 74 hpf to 120 hpf results in statistically significant increases in the number of S phase cells in the anterior intestine (Fig. 3C). There is an increase in S phase cells in the posterior intestine, but the increase is not statistically significant (Fig. 3C).

eNRSCs were again disrupted with DAPT between 74 hpf to 120 hpf, but grown to 11 dpf. There are significant increases in the number of S phase cells in both the anterior and posterior intestine (Fig. 3E) following incorporation of EdU on three separate days between 6 dpf to 11 dpf (experimental timeline Fig. 3D). Disruption of pNRSCs between 6 dpf to 11 dpf results in significant increases in proliferation both in anterior and posterior regions (Fig. 3G) following incorporation of EdU on three separate days between 6 dpf to 11 dpf (experimental timeline 3F). As proliferation is only in the interfold base epithelium between 5 dpf and 11 dpf (Li et al., 2019; Wallace and Pack, 2003), we find that both e and pNRSCs function to negatively regulate proliferation in the developing stem cell compartment.

Finally, we disrupted both eNRSCs (74 hpf to 120 hpf) and pNRSCs (6 dpf to 12 dpf) with EdU incorporation on three separate days between 6 dpf to 11 dpf (experimental timeline Fig. 3H). There are less significant changes in anterior number of cells in S phase than any of the other disruptions of e or pNRSCs (Fig. 3I). There are no significant increases in the number of S phase cells in the posterior region (Fig. 3I). Smaller increases in proliferation within the anterior intestine and decreased proliferation in the posterior intestine following disruption of both e and pNRSCs suggests that these two groups of NRSCs may work together to maintain proliferation at a set level during the first week post embryogenesis. e and pNRSCs may promote a portion of proliferation as well as inhibit the upper end of proliferation during the first week post embryogenesis.

3.6. The proliferative cell pool expands at the interfold base following NRSC disruption

Disruption of NRSCs increases the number of cells in S phase. Here we investigate whether increased cell numbers arise due to alteration of the cell cycle or recruitment of additional cells entering S phase. Following NRSC disruption the cell cycle may be shortened or cells that remain quiescent now reenter the cell cycle, increasing the number of cells in S phase. To identify how additional S phase cells arise following NRSC disruption, we performed the following two experiments.

The first experiment assays whether there are increases in the number of cells reentering S phase following NRSC disruption. Previously, we found that during the first two weeks post embryogenesis (6 dpf to 19

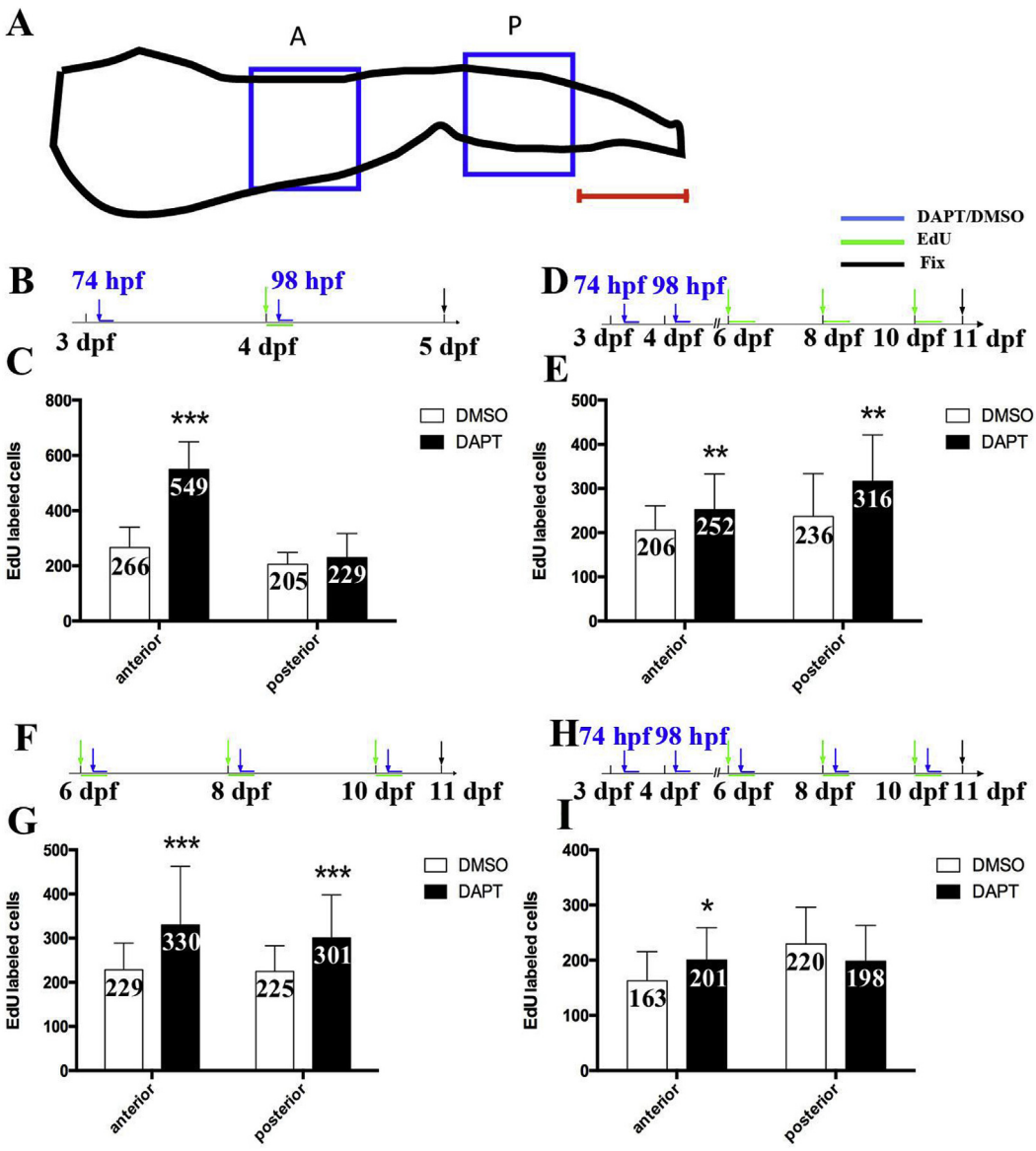

Fig. 3. Intestinal epithelial proliferation is up-regulated with developmental disruption of Notch receiving secretory cells (NRSCs). A. Diagram of anterior and posterior recorded regions (anterior end of intestine to left); one region (183 X 183 μm) in the anterior is where the intestine begins to enlarge in diameter (blue box labeled A) and the other in is in the posterior (blue box labeled P), which is 183 μm from the posterior end (indicated by red line). Time lines above each panel show timing of treatments and sample preparation (B, D, F, and H) as follows: green arrows indicate times of EdU addition, blue arrows are DAPT or DMSO control addition, black arrow is the end point of the experiment (sample preparation). DAPT disruption of NRSC development between 74 hpf to 120 hpf (C) demonstrates statistically significant difference in anterior proliferation at 120 hpf and an increase in the posterior compared to DMSO controls. When a group of fish exposed to DAPT between 74 hpf to 120 hpf and grown to 11 dpf (E), statistically significant increases in both the anterior and posterior are observed when compared to DMSO controls. Disruption of NRSC development for three (G) days with DAPT during the first week post-embryogenesis reveals statistically significant increases in epithelial proliferation in both anterior and posterior regions when compared to DMSO controls. Disruption of NRSC development during both the embryonic period (74 hpf to 120 hpf) and the first week post-embryogenesis (I) (DAPT applied for three separate days) results in increases in epithelial proliferation in the anterior. There is a decrease in proliferation in the posterior (I- not statistically significant). Average values are indicated in bars of graph. Student's t tests were performed between control and experimental groups. Values with significant differences between groups are indicated with an asterisk above the bar on the graph. The number of asterisks indicate differences with results lower than the indicated p value: *$p < 0.05$; **$p < 0.01$; ***$p < 0.001$. C. n=22; E. n=30; G. n=30; I. n=29.

dpf), most epithelial cells become quiescent after an initial division and do not enter further rounds of S phase (Li et al., 2019). Proliferation however continues throughout the first two weeks post embryogenesis as other cells then enter S phase and become quiescent following an initial division (Li et al., 2019). Following NRSC disruption, normally quiescent cells might re-enter the cell cycle, thereby increasing the number of cells in S phase. To determine whether increased numbers of interfold base epithelial cells re-enter the cell cycle, cells were labeled with two different nucleotides: EdU to identify cells initially in S phase, and then with BrdU to determine whether cells re-enter the cell cycle (experimental timeline Fig. 4A). Epithelial cells normally incorporate EdU and drop out of the cell cycle. If epithelial cells re-enter the cell cycle, they will also incorporate BrdU in a subsequent S phase and become co-labeled with both nucleotides.

To determine whether there are increased numbers of EdU and BrdU co-labeling cells we compared Notch disrupted individuals to DMSO controls during the first post embryonic week. While there are a few cells co-labeled in both DAPT and DMSO controls, the bulk of cells label with either EdU or BrdU only (Fig. 4B anterior and 4C posterior). There is a slight increase in co-labeled epithelial cells in NRSC disrupted

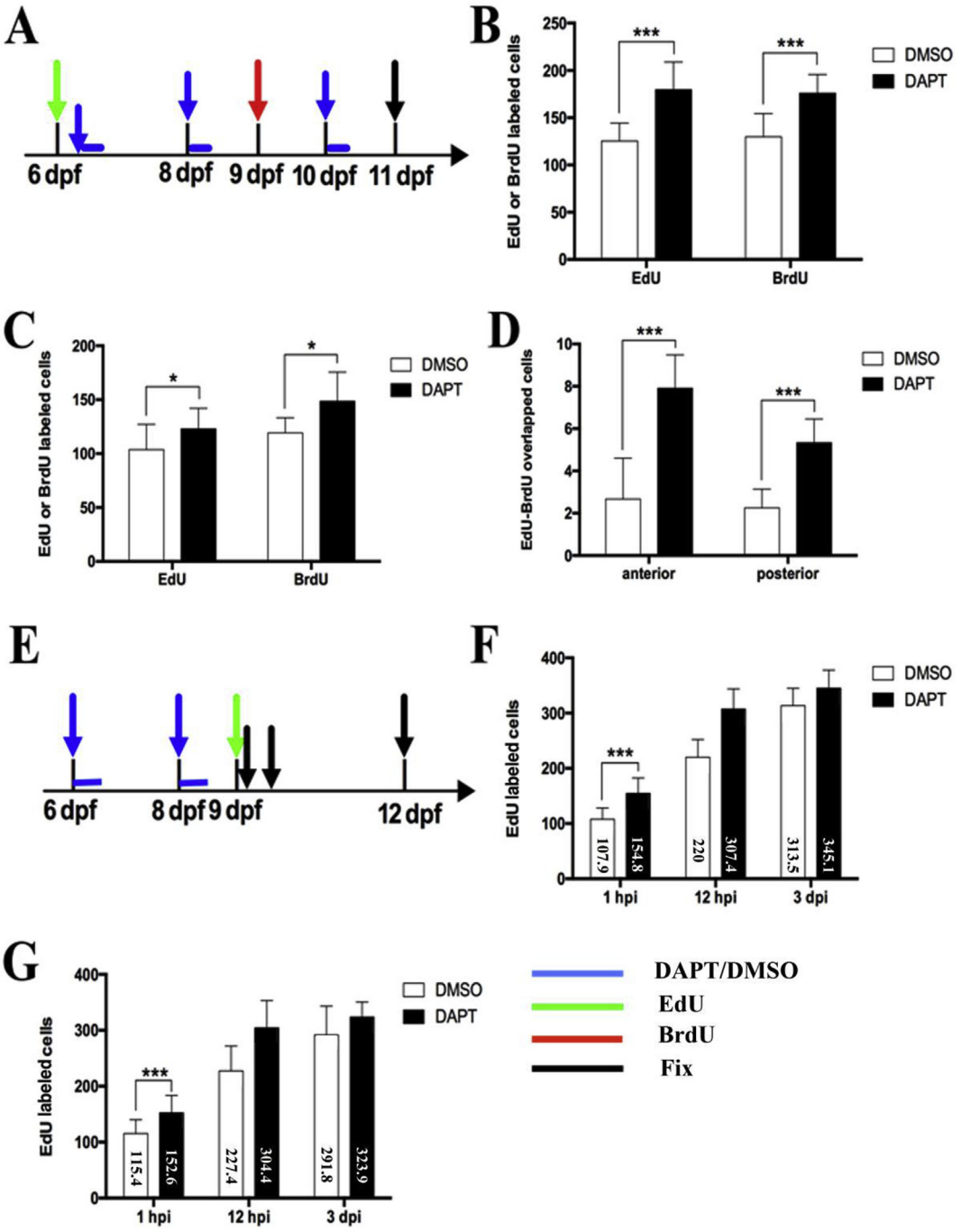

Fig. 4. Increased numbers of S phase cells due to disrupted NRSCs originate from newly recruited interfold base epithelial cells. NRSCs were disrupted with DAPT and compared to DMSO controls. Number of epithelial cells re-entering S phase was evaluated with a EdU incorporation followed by BrdU incorporation. Proliferation recorded in the anterior and posterior regions are the same as in Fig. 3A. Panel A shows the timeline; green arrow is time of EdU incorporation and red arrow is time of BrdU incorporation. Blue arrows indicate times of DAPT or DMSO addition and the black arrow is the end point. Significant increases in the number of cells in S phase occur in both the anterior (B) and posterior (C) with both EdU and BrdU incorporation. There are a few cells that incorporate both EdU and BrdU (D). Timeline in panel E evaluates both number of cells entering the cell cycle and the length of cell cycle. Individuals are exposed to either DAPT or DMSO at 6 dpf and 8 dpf (blue arrows), EdU was incorporated at 9 dpf. Individuals were stopped at 1 and 12 h as well as three days post EdU incorporation (indicated by three black arrows-first 1 h, second 12 h, and third 3 days). In both the anterior (F) and posterior (G), there is a significant increase in the number of initial cells recruited following NRSC disruption (anterior F and posterior G- 1 h post EdU injection-hpi). Both DAPT and DMSO controls double at the same rate (anterior F and posterior G- both at 12 dpi). Neither DAPT of DMSO individuals continues proliferating after the initial division as observed by a lack of statistically significant increases in EdU incorporated cells between 12 hpi and 3 dpi. Student's t tests were performed between control and experimental groups. Values with significant differences between groups are indicated with an asterisk above the bar on the graph. The number of asterisks indicate differences with results lower than the indicated p value: *$p < 0.05$; **$p < 0.01$; ***$p < 0.001$. B, C, D n=10; F, G n=20.

individuals that is statistically significant when compared to the DMSO control (Fig. 4D). As there are increased numbers of S phase cells in NRSC disrupted individuals, there is also likely to be an increase in the number of EdU and BrdU co-labeled cells compared to DMSO controls. NRSC disruption does not appear to allow quiescent cells reenter the cell cycle.

The second experiment identifies whether NRSC disruption results in overall higher numbers of cells in S phase at a given time and whether the speed of the cell cycle increases. A shortened cell cycle would allow more cells to be in S phase at a given time. Individuals are treated with DAPT or DMSO on 6 dpf and 8 dpf to disrupt NRSC development, followed by EdU incorporation (timeline 4E). To determine the number of cells in S phase at a given time, a group of individuals are labeled with EdU on 9 dpf. In one third of the EdU labeled individuals, EdU positive cells are recorded after an hour pulse at 9 dpf. Another third of the EdU labeled individuals are chased for 12 h while the last third are chased for 3 days (experimental timeline Fig. 4E). Comparing the number of EdU labeled cells between DAPT and DMSO controls following the one-hour pulse determines whether additional cells are recruited into S phase following NRSC disruption. The 12-h chase demonstrates whether the EdU labeled cells double. Previously, we determined that the cell cycle is about 12 h during the first week post embryogenesis and therefore we expect doubling of EdU labeled cells to occur during the first 12 h. The 3-day chase reveals whether EdU labeled cells continue to divide past the time that they double.

Counting labeled cells from the 1-h EdU pulse revealed that more cells are in S phase at a given time following DAPT disruption of NRSCs compared to the DMSO treatment (Fig. 4F anterior and 4G posterior). To determine the length of the cell cycle, the numbers of labeled cells following the EdU pulse were compared to numbers at the 12 h and 3 day chase periods. Completion of one cell cycle should produce approximately double the number of labeled cells when comparing the EdU pulse to chase. We find that in both DAPT and DMSO treatment groups, EdU labeled cells have doubled in number by 12 h following the original EdU pulse. This suggests that the cell cycle takes about 12 h in both NRSC disrupted individuals and DMSO controls (Fig. 4F anterior and 4G posterior). Also, during the three day chase period, there are no statistically significant increases in EdU labeled cells when comparing DAPT to DMSO controls. This experiment provides additional evidence that following NRSC disruption, epithelial cells entering the cell cycle remain quiescent following the initial cell cycle. These experiments indicate that interruption of NRSC development allows recruitment of additional epithelial interfold base cells into S phase, but does not increase the rate that cells go through the cell cycle or the number of cell cycle rounds. NRSCs may then play a role in limiting the field of epithelial interfold base cells that enter into the cell cycle at any given time.

3.7. Interruption of Wnt signaling down regulates Wnt target genes during both the end of embryogenesis and the first week post embryogenesis

We hypothesize that increased proliferation following NRSC disruption is due to up regulation of the level of Wnt signaling. In species as diverse as mammals, Drosophila and zebrafish, the Wnt signaling pathway has been shown to be critical in stimulating proliferation of epithelial cells in the stem cell niche (Barker, 2014; Cheesman et al., 2011; Haramis et al., 2006; Muncan et al., 2007; Neal et al., 2013; Tian et al., 2017). We first need to demonstrate that Wnt target genes will respond to disruption in Wnt signaling during the end of embryogenesis and the first week post embryogenesis. To disrupt Wnt signaling, we induced a transgenic line containing a dominant negative T-cell factor (TCF) (hsp70-TCFΔC) (DN TCF) (Martin and Kimelman, 2012). TCFs are required endpoint co-factors for recruitment of β-actin to activate Wnt target genes (Cadigan and Waterman, 2012).

Change in the level of Wnt signaling was identified through alteration of Wnt target gene expression using qPCR. We utilized the following Wnt target genes; *sox9b* (Blache et al., 2004; Cheesman et al., 2011), *NT1* (Cheesman et al., 2011; Kim et al., 2012), *myca* (Cheesman et al., 2011; He et al., 1998; Neal et al., 2013), *cyclinD1* (Neal et al., 2013; Tetsu and McCormick, 1999), *cdx1a* (Cheesman et al., 2011; Pilon et al., 2007), *axin2* (Cheesman et al., 2011; Lustig et al., 2002; Neal et al., 2013; Yan et al., 2001), and *ascl1b*.

While *ascl1b* was not previously shown to be a Wnt target gene, the gene has conserved synteny to the tetrapod homologue of *ascl2*, suggesting that *ascl1b* could serve as the *ascl2* homologue in teleosts (Ganz et al., 2014). The conserved synteny could make *ascl1b* a Wnt target gene. A previous report demonstrates increased *ascl1b* expression in *apc* mutants, suggesting *ascl1b* is a Wnt target gene. This may occur indirectly through overexpression of *stat3* and stimulation of the JAK/Stat pathway as chemical inhibition of the pathway (JAK/Stat) reduces *ascl1b* expression (Lin et al., 2011). *ascl1b* responds as a Wnt target but may not be a direct target.

Induction of the dominant negative (DN) TCF should reduce each of the relative Wnt target gene expression during embryogenesis and the first week post embryogenesis, but not other unrelated genes. To analyze alteration to Wnt signaling during embryogenesis, DN TCF individuals were heat shocked three times at 74 hpf, 94 hpf and 118 hpf followed by RNA isolation at 120 hpf (experimental timeline Fig. 5A). To analyze signaling during the first week post embryogenesis (6 dpf to 12 dpf), a group of DN TCF individuals were heat shocked on three different days (6 dpf, 8 dpf, and 10 dpf), followed by RNA isolation at 11 dpf (experimental timeline Fig. 5C). Expression levels of seven Wnt target genes (*sox9b*, *NT1*, *myca*, *cyclinD1*, *cdx1a*, *axin2*, and *ascl1b*) and an unrelated gene (Supplemental data Fig. S2) were compared between heat shocked DN TCF and heat shocked WT siblings by qPCR.

In both the embryonic and post-embryonic experiments, we find 1.89 to 2 fold reduction in expression of *ascl1b* compared to heat shocked WT siblings, suggesting that *ascl1b* responds to reductions in Wnt signaling and may be either a direct or indirect target of Wnt signaling (Fig. 5B and D). For the other Wnt target genes, we find reductions in a range from 1.19 to 2.78 fold when compared to heat shocked WT siblings (Fig. 5B and C). Reduction in the level of Wnt signaling then reduces expression of each of the selected Wnt target genes. As expression of the DN TCF is not continuous, we do not expect complete loss of Wnt target gene expression. We also suggest that other signaling pathways may contribute to a portion the Wnt target gene expression and prevent a more drastic reduction in expression levels.

3.8. Interruption of embryonic and post embryonic NRSCs results in increased Wnt target gene expression during post embryonic period, but not during the end of embryogenesis

To determine whether NRSC disruption results in increased Wnt signaling, we used qPCR to compare changes in Wnt target gene expression between NRSC disrupted individuals and DMSO treated controls. In these experiments, we used whole intestines and as a result, changes in gene expression may come from other sources such as mesenchymal and/or smooth muscle cells in addition to intestinal epithelial cells.

Here we disrupted eNRSCs (74 hpf to 120 hpf-analyzed at 11 dpf- Fig. 6C timeline) or pNRSCs (6 dpf to 11 dpf-analyzed 11 dpf- Fig. 6E timeline). We also disrupted eNRSCs (DAPT between 74 hpf to 120 hpf) but grew the individuals to 11 dpf (Fig. 6C timeline). Both eNRSCs (74 hpf to 120 hpf) and pNRSCs (6 dpf to 11 dpf- Fig. 6G timeline) were disrupted followed by analysis at 11 dpf.

Disruption of eNRSCs with analysis at the end of embryogenesis (120 hpf) results in no significant alteration in the relative expression levels of Wnt target genes when compared to DMSO controls (Fig. 6B). This suggests that eNRSCs do not change the level of Wnt signaling during the period between 74 hpf to 120 hpf even though we previously found that proliferation is upregulated following Notch inhibition during this period. This suggests that even though eNRSCs negatively regulate proliferation between 74 hpf to 120 hpf, they do not do so through Wnt signaling.

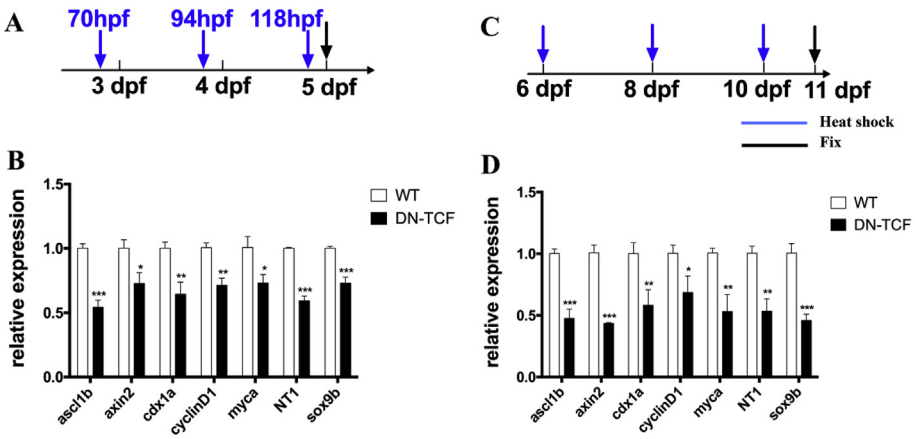

Fig. 5. Wnt transcription targets are down-regulated following DN-TCF expression. Wnt signaling is interrupted following heat shock expression of a dominant negative β-catenin transcription co-factor, TCF. During embryogenesis (timeline A), three heat shocks were performed at 70 hpf, 94 hpf and 118 hpf (blue arrows) and embryos analyzed at 120 hpf (black arrow). During the first week post-embryogenesis (timeline C), individuals were heat shocked three times at 6 dpf, 8 dpf and 10 dpf (blue arrows) and analyzed at 11dpf (black arrow). B, D: Histograms representing relative gene expression analyses via qPCR of the genes indicated (white bars for heat shocked wild-type controls, black bars for heat shocked DN TCF) at 74 hpf to 120 hpf (B) and during the first week post-embryogenesis (6 dpf to 12 dpf) (D). All seven of the observed target genes have statistically significant down-regulation (between 1.19 to 2.78 fold) relative to heat shocked WT siblings during both embryonic period and post embryonic period. Student's t tests were performed between control and experimental groups. Values with significant differences between groups are indicated with an asterisk above the bar on the graph. The number of asterisks indicate differences with results lower than the indicated p value: *$p < 0.05$; **$p < 0.01$; ***$p < 0.001$.

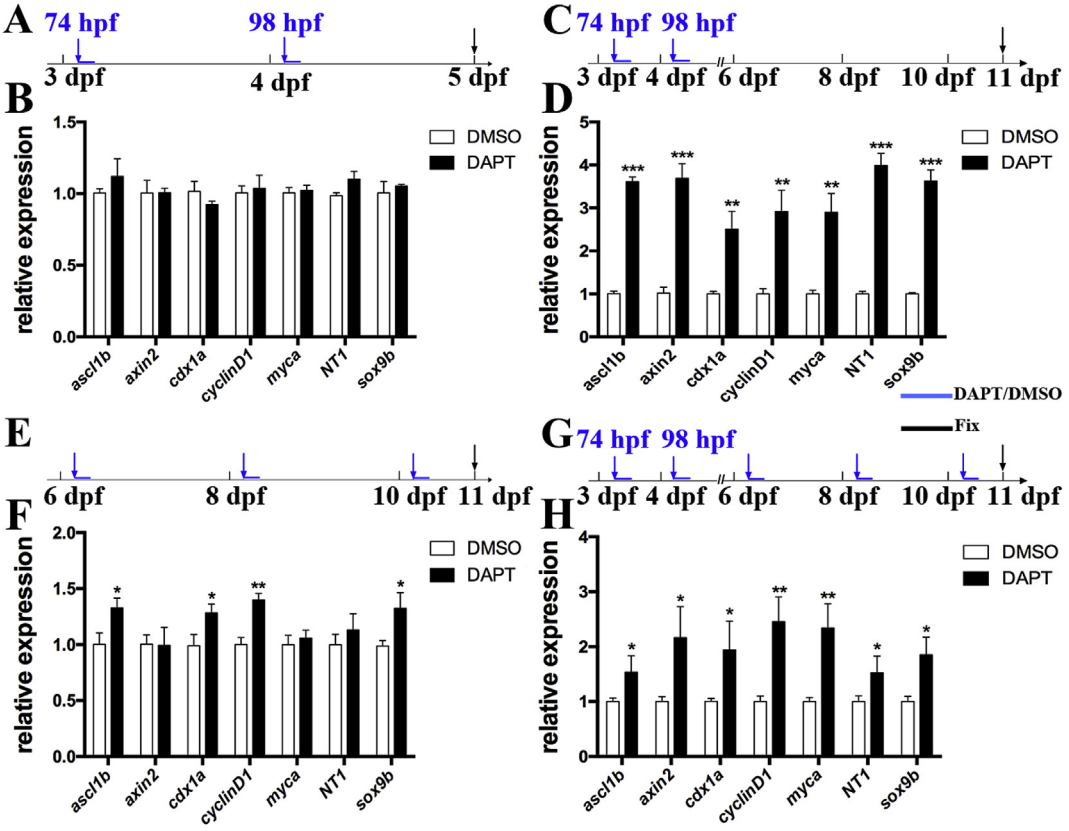

Fig. 6. Wnt transcription targets are up-regulated following DAPT disruption of NRSCs during the first week of the post-embryonic period. Disruption of NRSCs with DAPT were performed in a similar time frame to analysis of epithelial proliferation levels (Fig. 3). Relative gene expression of disrupted NRSCs was compared to DMSO controls using qPCR. Timelines (A, C, E and G) show time of DAPT or DMSO control exposures (blue arrows) followed time of analysis (black arrow). (B) Application of DAPT between 74 hpf to 120 hpf does not show significant changes in Wnt target gene expression at 120 hpf when compared to DMSO treated controls (D). Significant changes in all target genes occur when embryos are treated with DAPT between 74 hpf to 120 hpf and grown to 11 dpf (comparing histogram in B to histogram in D). (F) Disruption of NRSC development with DAPT during the first week of the post-embryonic period reveals increased expression in four Wnt target genes. (H) Disruption of NRSC development in both embryonic and post-embryonic periods using DAPT significantly increases expression of all Wnt target genes. Student's t tests were performed between control and experimental groups. Values with significant differences between groups are indicated with an asterisk above the bar on the graph. The number of asterisks indicate differences with results lower than the indicated p value: *$p < 0.05$; **$p < 0.01$; ***$p < 0.001$.

The eNRSCs formed between 74 hpf to 120 hpf do however alter the level of Wnt signaling during the first week post embryogenesis. Disruption of eNRSCs with analysis at 11 dpf (Fig. 6D) results in increased expression of all seven of the analyzed Wnt target genes. This suggests that even though eNRSCs do not alter Wnt signaling during embryogenesis, they are capable of altering Wnt signaling during the post embryonic period. Disruption of only pNRSCs results in up regulation of only four of the seven Wnt target genes (Fig. 6F). Up regulation of these four Wnt target genes may be all that is required to increase proliferation. In these experiments, we observe differential regulation of Wnt target genes from no alteration, a few targets altered, or all targets altered. We suggest that e and pNRSCs may be able to differentially regulate Wnt targets by acting on alternate target gene enhancers, which could be differentially modified. Previously, differential expression of Wnt target genes has been shown to be due to differential chromatin marks and occupancy of TCF in the enhancer region (Wohrle et al., 2007). Modification of target gene enhancers in different cells could then produce varied responses of target genes to Wnt signaling. Enhancers could then be further modified over development, producing additional changes in Wnt target response.

3.9. Interruption of Notch signaling alters expression of EGF and IGF receptors and ligands

Epithelial proliferation is increased following disruption of NRSCs in each of the combinations that were investigated. Even though proliferation is increased at the end of embryogenesis following eNRSC disruption, we find no increase in Wnt target genes. We suggest that eNRSCs downregulate epithelial proliferation though a signaling pathway other than Wnt.

Both Epidermal Growth Factor (EGF) (Farin et al., 2012; Sato et al., 2011) and Insulin-Like Growth Factor (IGF) (Bortvedt and Lund, 2012; Van Landeghem et al., 2015) pathways drive proliferation of epithelial stem cells. Following resection of the adult zebrafish intestine, proliferation increases in the following two weeks with a corresponding upregulation of EGF and IGF pathway components similar to mammalian models of short bowel syndrome (Schall et al., 2015). Both EGF and IGF signaling pathways are active and promote proliferation in the adult zebrafish intestine. Therefore, EGF and IGF pathways may play a role in driving increased levels of proliferation between 74 hpf to 120 hpf following eNRSC disruption.

Using qPCR, we compared relative expression levels of EGF and IGF ligand and receptor genes between individuals following NRSC disruption to DMSO controls. Similar to the analysis of the Wnt target genes, we applied DAPT or DMSO in the same four time frames as with analysis of proliferation levels. eNRSCs were disrupted with analysis at 120 hpf (Fig. 7A) or 11 dpf (Fig. 7C). pNRSCs were disrupted with analysis at 11 dpf (Fig. 7E). Also both eNRSCs and pNRSCs were disrupted with analysis at 11 dpf (Fig. 7G).

We find both increases and decreases in EGF and IGF pathway

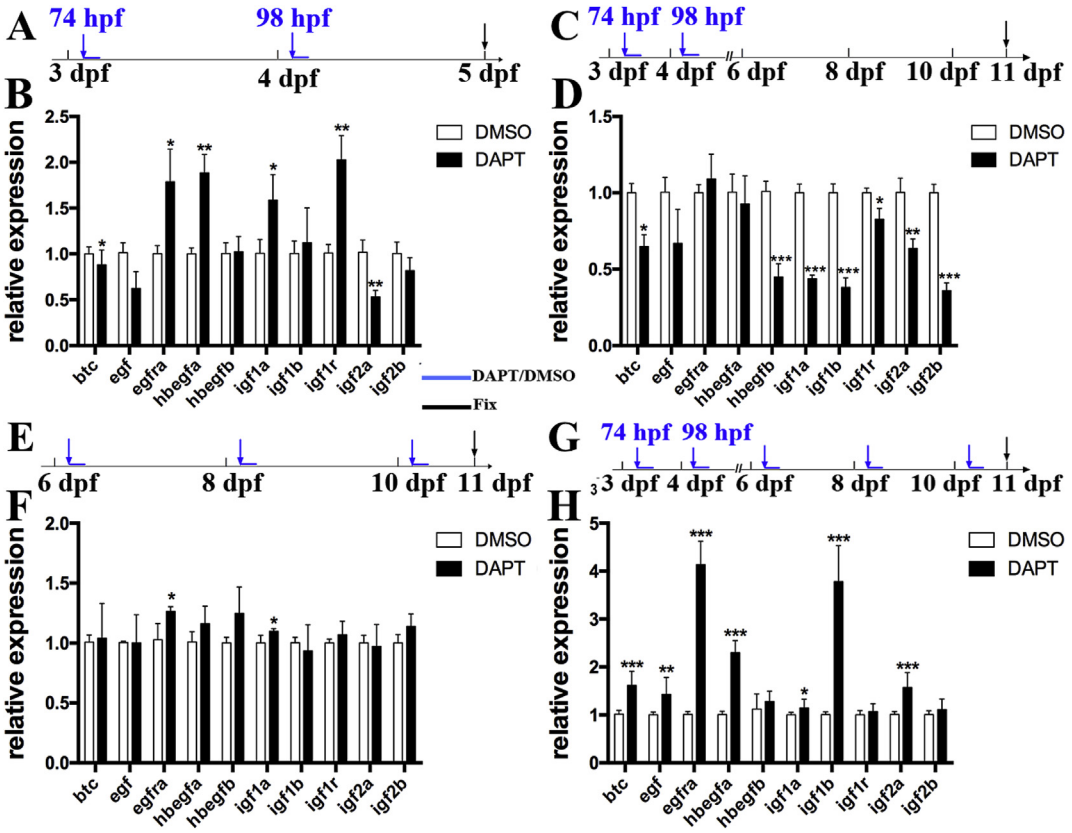

Fig. 7. EGF and IGF pathways are mis-regulated following DAPT disruption of NRSCs during embryonic and post-embryonic periods. NRSC disruption with DAPT was performed in a similar manner to both proliferation (Fig. 3) and Wnt target analysis (Fig. 6). Timelines for these experiments (A, C, E and G) are shown in the panel above the experiment. DAPT or DMSO control exposure times are shown (blue arrows) followed by time of analysis (black arrow). qPCR was used to assay relative gene expression between DAPT and DMSO controls. DAPT exposure at 74 hpf and 98 hpf followed by analysis at 120 hpf (timeline A) results in up-regulation of EGF and IGF ligands and receptors with down-regulation of one EGF and two IGF ligands at 120 hpf (B). Following embryonic DAPT treatment (74 hpf to 120 hpf) with analysis at 11 dpf (timeline C), EGF ligands are down-regulated and both IGF receptor and ligands are down-regulated (D). DAPT treatment during the first week post-embryogenesis (timeline E) results in up-regulation of one EGF receptor and one IGF ligand (F). DAPT treatment during both embryogenesis and the first post-embryonic week (timeline G) results in up-regulation of EGF receptor and ligands as well as IGF ligands (H). Student's t tests were performed between control and experimental groups. Values with significant differences between groups are indicated with an asterisk above the bar on the graph. The number of asterisks indicate differences with results lower than the indicated p value: *$p < 0.05$; **$p < 0.01$; ***$p < 0.001$.

components depending on the combination of NRSCs that are disrupted. Following disruption of eNRSCs with analysis at 120 hpf (timeline Fig. 7A), we find between 1.5 to 2 fold increases in the relative expression of *egfra*, *hb-egfa*, *igf1a*, and *igf1r* genes (Fig. 7B), suggesting that eNRSCs down regulate epithelial proliferation in part by downregulating both the EGF and IGF signaling pathways. While there is reduction in the relative expression of *egf*, *igf2a* and *igf2b* genes during the same period, these ligands may not be involved in promoting proliferation.

In contrast, when eNRSCs are disrupted (but not pNRSCs) and analyzed at 11 dpf (timeline Fig. 7C), there are decreases in the relative expression of *btc*, *egf*, *hbegfb* ligand genes as well as all the genes of the *igf* ligands and receptors (Fig. 7D). We suggest that in the absence of eNRSCs, pNRSCs are able to cause a more substantial down regulation of EGF and IGF pathways (Fig. 7D). eNRSCs may play a role in supporting proliferation during the first week post embryogenesis. eNRSCs would then have a dual role in down regulating EGF and IGF pathway expression during the end of embryogenesis but may also support a level of EGF and IGF pathway component expression during the first week post embryogenesis. Without eNRSCs to support EGF and IGF pathway expression during the first week post embryogenesis, the pNRSCs would be able to have a more unchecked downregulation of the EGF and IGF signaling pathways.

When pNRSCs are disrupted (but not eNRSCs) and analyzed at 11 dpf (timeline Fig. 7E), only *egfra* and *igf1a* are marginally increased (Fig. 7E). In this experiment, we suggest that disruption of pNRSCs prevents the normal downregulation of EGF and IGF signaling at the beginning of the first week post embryogenesis. eNRSCs here may be exerting a secondary role in maintaining EGF and IGF pathway expression during the first week post embryogenesis. However, when both e and pNRSCs are disrupted (timeline 7G), most ligands and receptors have significant increases except for *igf1r* and *igf2b* (Fig. 7H). We suggest that loss of eNRSCs results in increased ligand and receptor expression during the end of embryogenesis (74 hpf to 120 hpf). Elevated EGF and IGF expression would normally be downregulated by pNRSCs between the end of embryogenesis and the first week post embryogenesis. In this experiment, we suggest that high levels of EGF and IGF expression continues into the post embryonic period due to a lack of pNRSCs which would normally reduce EGF and IGF expression. pNRSCs may then play a role in reduction of EGF and IGF signaling at the end of embryogenesis to allow Wnt signaling to become the primary driver of proliferation during the post embryonic period.

3.10. Wnt, EGF and IGF signaling play differing roles in driving intestinal epithelial proliferation as the intestine develops

We hypothesize that inhibition of the prominent signaling pathway driving epithelial proliferation will reduce increased epithelial proliferation due to NRSC disruption. qPCR results demonstrate that the EGF and IGF are prominent signaling pathways driving epithelial proliferation during embryogenesis (74 hpf to 120 hpf). This changes during the transition between the end of embryogenesis (120 hpf) and the first week post embryogenesis (6 dpf to 12 dpf) when Wnt signaling becomes the prominent driver of epithelial proliferation.

Here we inhibit each signaling pathway in both NRSC disrupted and DMSO control individuals during the embryonic period and the first week post embryonic period. Changes in proliferation are assayed following EdU incorporation. To inhibit Wnt signaling we used the dominant negative (DN) TCF (Martin and Kimelman, 2012). EGF signaling was inhibited with the cell-permeable EGF kinase inhibitor AG-1478. (Budi et al., 2008). IGF was inhibited with NVP-AEW541 (Chablais and Jazwinska, 2010).

We first inhibited Wnt signaling during the embryonic period and first week post embryonic period. qPCR results suggest that Wnt inhibition during the embryonic period will not affect epithelial proliferation. We expressed DN TCF between 74 hpf to 120 hpf either on its own or following DAPT addition to disrupt eNRSC development (experimental timeline Fig. 8A). As expected, expression of DN TCF does not reduce epithelial proliferation (Fig. 8B), even though DN TCF expression at this stage reduces expression of Wnt target genes (Fig. 5B). In contrast, when either AG-1478 (EGF inhibitor) (timeline Fig. 8C) or NVP-AEW541 (IGF inhibitor) (timeline Fig. 8E) is added on its own during the embryonic period, proliferation is reduced in both the anterior and posterior regions below WT levels (Fig. 8D- EGF or F- IGF). For both inhibitors, we have performed internal controls using previously identified EGF and IGF targets to demonstrate the specificity of the inhibitors (Supplemental Information Fig. S3 EGF; S4 and S5 IGF). With addition of DAPT to inhibit development of eNRSCs, epithelial proliferation increases as before (Fig. 8D and F and Fig. 3). When DAPT is combined with either of the inhibitors, the epithelial proliferation rate is reduced to almost WT levels (Fig. 8D or F). While the level of epithelial proliferation might be expected to drop below WT levels with either the EGF or IGF inhibitor, the opposite signaling pathway is likely preventing a more severe reduction in proliferation. We are able to reduce proliferation through EGF and IGF but not Wnt inhibition following eNRSC disruption. These results support the qPCR observation that increases in EGF and IGF signaling are primarily responsible for driving both normal epithelial proliferation and increases in epithelial proliferation resulting from disruption of eNRSCs during embryogenesis.

In contrast to the embryonic period, when Wnt signaling is inhibited during the first week post embryogenesis, epithelial proliferation is significantly reduced. DN-TCF was expressed with three heat shocks on 6 dpf, 8 dpf and 10 dpf during the first week post-embryogenesis. EdU was incorporated on the same 3 day s as the heat shocks to determine changes in epithelial proliferation (timeline Fig. 9A). The number of EdU labeled cells are significantly reduced below control heat shocked siblings without the DN-TCF construct levels (Fig. 9B). Disruption of pNRSCs following DAPT treatment on 6 dpf, 8 dpf and 10 dpf, as before, increases epithelial proliferation (Figs. 9B–3G). Increased epithelial proliferation resulting from pNRSC disruption is reduced to near WT levels following Wnt inhibition with DN-TCF (Fig. 9B). Reduction of S phase numbers below DMSO control numbers is likely prevented by other signaling pathways promoting epithelial proliferation. Both qPCR and signal inhibition data support a role for EGF and IGF signaling as a prominent driver of epithelial proliferation during embryogenesis, followed by a switch to Wnt signaling during the post-embryonic phase. We also find that increases in proliferation following NRSC disruption is driven by the prominent signaling pathway promoting proliferation during the respective period (EGF and IGF in embryonic and Wnt in post embryonic).

4. Discussion

Here we identify a subset of intestinal epithelial secretory cells that are interspersed among proliferative cells at the developing fold base. The NRSCs co-localize with the pan-secretory marker 2F11 suggesting that they are secretory cells. These secretory cells receive Notch signaling after the period of specification between enterocytes and secretory cell lineages. We suggest that Notch signaling is required for differentiation of these secretory cells (referred to as Notch receiving secretory cells-NRSCs). NRSCs begin forming after 74 hpf. New NRSCs continue differentiating throughout the first week post-embryogenesis. We find low level *nkx2.2a* co-localization with NRSCs suggesting they are enteroendocrine cells.

NRSCs may be conserved across multiple vertebrate species. Previously, a search was performed to identify conserved accessible chromatin regions specific to intestinal epithelial cells across a number of vertebrates (zebrafish, stickleback, mouse and human) (Lickwar et al., 2017). While common accessible chromatin regulatory regions active primarily in intestinal epithelial cells are conserved across vertebrate species, they often do not retain sequence conservation (Lickwar et al., 2017). However, among the conserved accessible chromatin regulatory regions, a highly conserved sequence for the *her6/hes1* gene, which is active in a

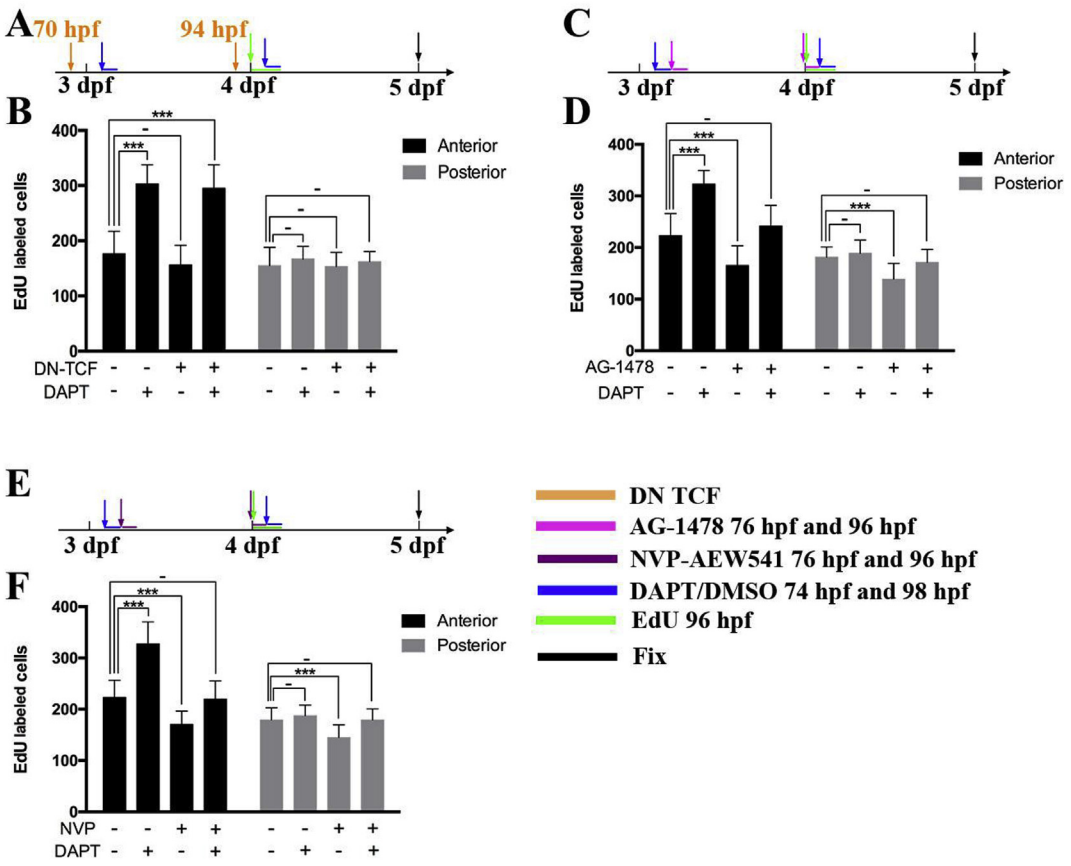

Fig. 8. Inhibition of either EGF or IGF pathways but not Wnt signaling inhibition reduces embryonic intestinal epithelial proliferation. Timeline of experiments are outlined for DN TCF (A), EGF (C) and IGF (E). Heat shock times are shown with orange arrows (A) or inhibitor addition (pink arrow- C or brown arrows-E) Each inhibitor was used for a 2-h exposure. Blue arrows in each figure are DAPT or DMSO control additions (2-h exposure), green arrows are time of EdU incubation (4 h) and black arrow is the end of the experiment. Anterior and posterior regions recorded in these experiments are the same areas indicated in Fig. 3A. Inhibition of Wnt signaling with the dominant negative (DN) TCF results in no statistically significant reductions in epithelial proliferation in either the anterior or posterior (B). Addition of DAPT (B) to disrupt NRSCs increases anterior epithelial proliferation as in Fig. 3. DAPT increases in proliferation are not reduced in either anterior or posterior regions following inhibition of the Wnt pathway with DN TCF expression (B). Inhibition of the EGF pathway using the cell-permeable EGF kinase inhibitor AG-1478 EGF (D) or the IGF inhibitor NVP-AEW541 (F) both reduce epithelial proliferation by a statistically significant value compared to WT. When DAPT is added to disrupt NRSCs, epithelial proliferation is again increased while addition of both DAPT and AG-1478 (D) or DAPT and NVP-AEW541 (F) reduces DAPT induced proliferation almost back to WT levels in both the anterior and posterior. B. DMSO n=20, DAPT n=21, DMSO-DN TCF n=28, DAPT-DN TCF n=20; D. DMSO-DMSO n=23, DAPT-DMSO n=24, AG-1478-DMSO n=28, AG-1478-DAPT n=26; F. DMSO-DMSO n=27, DAPT-DMSO n=27, NVP-AEW541-DMSO n=27, NVP-AEW541-DAPT n=28. Analyzed using one way analysis of variance (ANOVA) $p < 0.001$ B anterior: $F(3,84) = 91.86$, $P=0$; posterior: $F(3,84) = 1.42$, $p = 0.24$ D anterior: $F(3,97) = 78.45$, $p=0$; posterior; $F(3,97) = 18.98$, $p=0$ F anterior: $F(3,105) = 96.48$, $p=0$ posterior: $F(3,105) = 18.52$, $p=0$. All means were found to not be equal except for the posterior group in panel B. Significant differences from the untreated group were determined using the Student's *t*-test with Bonferroni correction and indicated with asterisks above the bars, ***$p < 0.0001$.

population of Notch positive cells, was identified and contains the RBPJ binding site required for *her6/hes1* expression in zebrafish intestinal epithelial cells. Furthermore, the corresponding human sequence also drives expression in a group of zebrafish Notch positive intestinal epithelial cells (Lickwar et al., 2017). Notch appears to act on an enhancer that is active and highly conserved in intestinal epithelial cells, suggesting that NRSCs may have conserved function in development of the intestines of diverse vertebrate species.

Interruption of NRSC development both in the embryonic period (74 hpf to 120 hpf) and the first week post embryonic period (6 dpf to 12 dpf) increases proliferation rates of immature stem cells at the interfold base, suggesting that NRSCs negatively regulate epithelial proliferation. With interruption of NRSC development, there are corresponding changes in signaling pathways involved in promotion of epithelial proliferation. We find that increased proliferation during the first week post embryogenesis is promoted by Wnt signaling, as e and pNRSC disruption increases expression of Wnt target genes. Also, Wnt pathway inhibition reduces increased proliferation rates following NRSC disruption during the first week post embryogenesis (6 dpf to 12 dpf). Both upregulation of Wnt target genes and reduction of proliferation following Wnt inhibition suggests that Wnt signaling promotes intestinal epithelial proliferation during the first week post embryogenesis. These experiments also suggest that increases in epithelial proliferation following disruption of e and pNRSCs is driven by increased Wnt signaling during the first week post embryogenesis.

While Wnt signaling promotes intestinal epithelial proliferation during the first week post embryogenesis, eNRSC disruption does not alter Wnt target genes during embryogenesis. Also, Wnt pathway inhibition does not reduce the increased proliferation following NRSC disruption during embryogenesis. These experiments suggest that Wnt signaling does not promote intestinal epithelial proliferation during embryogenesis. Instead, Wnt signaling only begins to promote epithelial proliferation during the transition between the embryonic and post embryonic period.

As Wnt signaling does not appear to promote proliferation during the embryonic period, we investigated whether other signaling pathways might play this role. A number of pathways contribute to drive proliferation in mammals including contributions from the EGF (Farin et al.,

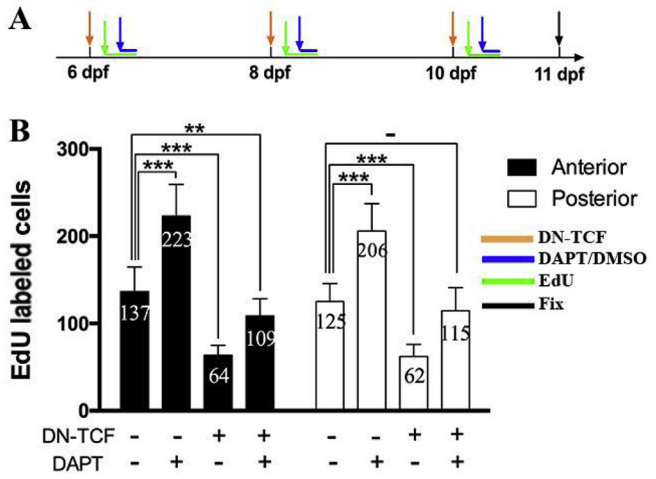

Fig. 9. Inhibition of Wnt signaling during the first week post-embryogenesis reduces epithelial proliferation. Timeline of experiment is outlined in A. Orange arrows indicate times of heat shock, green arrows indicate times of EdU incubation, and blue arrows indicate times of DAPT or DMSO treatment. Recorded anterior and posterior regions are the same areas indicated in Fig. 3A. B. Inhibition of Wnt signaling through DN-TCF expression during the first post embryonic week significantly reduces epithelial proliferation in both anterior and posterior regions. With the combination of DAPT (to inhibit NRSC development) and expression of DN-TCF (to inhibit Wnt signaling), proliferation levels are reduced to WT levels in both anterior and posterior regions. DMSO n=28; DAPT n=23; DN-TCF-DMSO n=29; DN-TCF-DAPT n=28. Groups of individuals were analyzed using one way analysis of variance (ANOVA) $p < 0.001$ B anterior: $F(3,104) = 184.2$, $p=0$; posterior $F(3,104) = 159.95$, $p=0$. All means were found to be unequal. Significant differences from the untreated group were determined using the Student's *t*-test with Bonferroni correction and indicated with asterisks above the bars, $^{**}p < 0.001$; $^{***}p < 0.0001$.

2012; Sato et al., 2011) and IGF (Bortvedt and Lund, 2012; Van Landeghem et al., 2015) pathways. EGF and IGF have also been demonstrated to play a role in proliferation increases following resection of the adult zebrafish intestine (Schall et al., 2015). Following disruption of embryonic NRSCs there are increases in the relative gene expression of EGF and IGF receptors and ligands. In addition when either EGF or IGF signaling pathways are inhibited following embryonic NRSC disruption, increased proliferation levels are reduced. EGF and IGF pathways play a role in promotion of proliferation during embryogenesis. The increased epithelial proliferation following disruption of eNRSCs is driven by increased EGF and IGF signaling at the end of embryogenesis.

We find that pNRSCs play a role in reduction of EGF and IGF signaling during the transition between embryogenesis and the first week post embryogenesis. When only embryonic NRSCs are disrupted but post embryonic NRSCs are allowed to develop, decreased expression of EGF and IGF receptors and ligands is observed during the first week post embryogenesis. Because the post embryonic NRSCs are still present, we suggest that post embryonic NRSCs play a role in reduction of the level of EGF and IGF pathways. Reduction of EGF and IGF pathways may help to mediate transition to Wnt signaling as the predominant pathway driving epithelial proliferation at the beginning of the first week post embryogenesis. We suggest that EGF and IGF signaling needs to be downregulated before Wnt signaling is upregulated. Promotion of epithelial proliferation may not be compatible with concurrent activation of all signaling pathways.

We propose the following model for formation of the intestinal epithelial stem cell compartment and regulation of proliferation within the developing niche. During the end of embryogenesis, there is a restriction of proliferation to the interfold base, which appears to be completed by the end of embryogenesis (120 hpf) (Wallace et al., 2005a). Here we find that restriction of proliferation to the interfold base is coincident with a shift from EGF and IGF driving epithelial proliferation to Wnt signaling being the main driver of proliferation. We suggest that this may be a period when an immature stem cell niche is established. This potential niche would still need to undergo multiple changes before reaching the mature form.

In this model, as the immature stem cell niche develops, the majority of secretory cells at the interfold base would be involved in positive regulation of proliferating cells (represented by green secretory cells in Fig. 10A and C designated as EE). Embryonic EE cells (labeled as green EE cells in Fig. 10A) would promote proliferation primarily through EGF and IGF signaling (larger blue bar in Fig. 10A), with some contribution by Wnt during embryogenesis (smaller red bar in Fig. 10A). During the transition from embryogenesis to the first week post embryogenesis (6 dpf to 12 dpf), post embryonic EE cells would promote proliferation primarily through Wnt signaling which becomes the primary driver of epithelial proliferation (switch between height of blue EGF and IGF and red bars Wnt indicting change in signaling pathway dominance - Fig. 10C).

The NRSCs (represented by both red eNRSCs in Fig. 10B and D and the yellow pNRSCs in Fig. 10D) would play a role in counteracting the activity of the EE cells by restricting proliferation to prevent epithelial cells from over proliferating. With development of the embryonic NRSCs (labeled as red eNRSCs in Fig. 10B) there is a reduction in the top end of epithelial proliferation through reduction of EGF and IGF signaling (reduced blue bar in Fig. 10B as compared to the larger blue bar in 10A without eNRSCs).

pNRSCs would play a role in downregulating Wnt signaling during

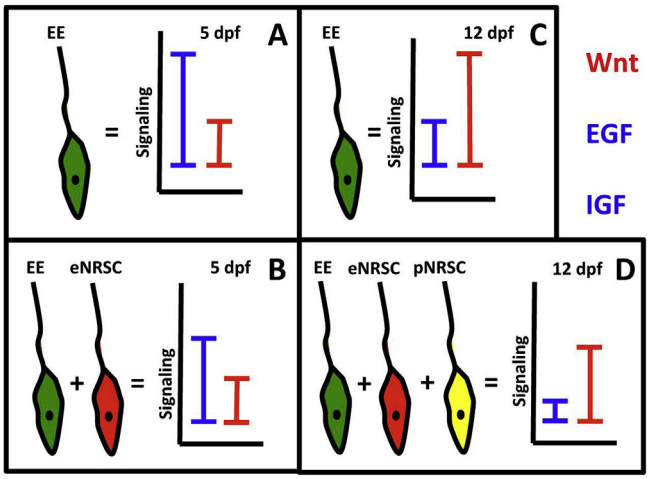

Fig. 10. Model for regulation of intestinal epithelial proliferation. We suggest that the more numerous enteroendocrine cells associated with proliferating cells are positive drivers of proliferation (green cell labeled EE). Without NRSCs, there would be higher levels of EGF, IGF and Wnt signaling as well as higher proliferation rates (A). There are two types of NRSCs, one of which forms during the embryonic period (red cell labeled eNRSC-B and D) and the other during the first week post-embryonic period (yellow cell labeled pNRSC- D). The embryonic NRSCs (eNRSC) reduce the upper end of both EGF and IGF signaling. Reducing EGF and IGF signaling reduces the number of epithelial cells recruited into S phase during embryogenesis. eNRSCs do not appear to alter Wnt signaling during embryogenesis (B) but reduce Wnt signaling later during the first week post embryogenesis (D). pNRSCs reduce the upper end of Wnt signaling and consequently the number of epithelial cells recruited into S phase during the first week post embryogenesis (D). As the major signaling pathways driving proliferation change from EGF/IGF to Wnt between embryogenesis and the post embryonic period, NRSCs would then play a role in this switch. pNRSCs appear to dramatically reduce both EGF and IGF signaling during the first post embryonic week. Downregulation of EGF and IGF signaling may be necessary to allow for Wnt signaling to become the prominent driver of epithelial proliferation during the first week post embryogenesis. We suggest that high levels of both signaling pathways are not compatible with each other to drive epithelial proliferation. Both groups of NRSCs however are involved in downregulating the upper end of the signaling driving proliferation. Other signaling pathways are likely to be involved in stimulation of epithelial proliferation during each of these periods but were not investigated in this study.

the first week post embryogenesis to place an upper limit on the number of cells produced during epithelial proliferation. pNRSC limiting Wnt signaling is represented in the difference between higher levels of Wnt signaling (Fig. 10B red bar) with only EE cells and the lower level of Wnt signaling (Fig. 10C red bar) with e and pNRSCs. Both e and pNRSCs play a role in Wnt downregulation during the post embryonic period.

We suggest that pNRSCs also aid in transition to the immature stem cell niche between the end of embryogenesis and the first week post embryogenesis. Development of post embryonic NRSCs (labeled as yellow pNRSCs in Fig. 10D) would promote a dramatic reduction in EGF and IGF signaling (smaller blue bar in Fig. 10D as compared to the larger blue bar in Fig. 10C without e or pNRSCs). This would promote transition to the predominance of Wnt signaling at the beginning of the post embryonic period. Addition of pNRSCs with EE cells results in reduced EGF and IGF signaling when compared to higher levels of signaling in Fig. 10C were there is only EE cells. Each group of secretory cells would then play a role in either up or down regulation of signaling pathways driving proliferation. The overall function of NRSCs would be to perform varying degrees of down regulation of signaling. eNRSCs may also prevent epithelial proliferation from dropping too low. During the first week post embryogenesis, the eNRSCs and pNRSCs may interact and regulate proliferation in ways that one group alone will not be able to perform.

We have identified and begun to characterize a subset of intestinal secretory cells (Notch receiving secretory cells- NRSCs) that restrict proliferation levels within the developing intestinal stem cell compartments. These secretory cells limit the pool of proliferative epithelial cells by restricting levels of at least three pathways that drive epithelial proliferation (Fig. 10). These secretory cells are likely conserved in vertebrate evolution (Lickwar et al., 2017). Restriction of intestinal epithelial proliferation by NRSCs during development may be a common mechanism across many vertebrate species.

Acknowledgments

The authors would like to thank Michael Parsons for providing the following lines: *Tg(T2KTp1glob:creER^{T2})^{jh12}*, *Tg(T2Kβactin:loxP-stop-loxP-hmgb1-mCherry)^{jh1}*, *Tg[nkx2.2a:mEGFP]*. The authors would like to thank Benjamin L. Martin for providing the dominant negative TCF line: Tg(HS:TCFΔC)^{W74}. Research reported in this publication was supported by the Eunice Kennedy Shriver National Institute of Child Health & Human Development of the National Institutes of Health under Award Number R15HD088202. Part of the qPCR was supported by the NIH award 1R15GM1131-01 to CFH. The content is solely the responsibility of the authors and does not necessarily represent the official views of the National Institutes of Health.

Appendix A. Supplementary data

Supplementary data to this article can be found online at https://doi.org/10.1016/j.ydbio.2019.08.005.

References

Barker, N., 2014. Adult intestinal stem cells: critical drivers of epithelial homeostasis and regeneration. Nat. Rev. Mol. Cell Biol. 15, 19–33.
Bezencon, C., Furholz, A., Raymond, F., Mansourian, R., Metairon, S., Le Coutre, J., Damak, S., 2008. Murine intestinal cells expressing Trpm5 are mostly brush cells and express markers of neuronal and inflammatory cells. J. Comp. Neurol. 509, 514–525.
Bjerknes, M., Khandanpour, C., Moroy, T., Fujiyama, T., Hoshino, M., Klisch, T.J., Ding, Q., Gan, L., Wang, J., Martin, M.G., Cheng, H., 2012. Origin of the brush cell lineage in the mouse intestinal epithelium. Dev. Biol. 362, 194–218.
Blache, P., van de Wetering, M., Duluc, I., Domon, C., Berta, P., Freund, J.N., Clevers, H., Jay, P., 2004. SOX9 is an intestine crypt transcription factor, is regulated by the Wnt pathway, and represses the CDX2 and MUC2 genes. J. Cell Biol. 166, 37–47.
Bortvedt, S.F., Lund, P.K., 2012. Insulin-like growth factor 1: common mediator of multiple enterotrophic hormones and growth factors. Curr. Opin. Gastroenterol. 28, 89–98.
Budi, E.H., Patterson, L.B., Parichy, D.M., 2008. Embryonic requirements for ErbB signaling in neural crest development and adult pigment pattern formation. Development 135, 2603–2614. Cambridge, England.
Cadigan, K.M., Waterman, M.L., 2012. TCF/LEFs and Wnt signaling in the nucleus. Cold. Spring. Harbor. Perspect. Biol. 4.
Chablais, F., Jazwinska, A., 2010. IGF signaling between blastema and wound epidermis is required for fin regeneration. Development 137, 871–879.
Cheesman, S.E., Neal, J.T., Mittge, E., Seredick, B.M., Guillemin, K., 2011. Epithelial cell proliferation in the developing zebrafish intestine is regulated by the Wnt pathway and microbial signaling via Myd88. Proc. Natl. Acad. Sci. U. S. A 108 (Suppl. 1), 4570–4577.
Crosnier, C., Vargesson, N., Gschmeissner, S., Ariza-McNaughton, L., Morrison, A., Lewis, J., 2005. Delta-Notch signalling controls commitment to a secretory fate in the zebrafish intestine. Development 132, 1093–1104. Cambridge, England.
Desai, S., Loomis, Z., Pugh-Bernard, A., Schrunk, J., Doyle, M.J., Minic, A., McCoy, E., Sussel, L., 2008. Nkx2.2 regulates cell fate choice in the enteroendocrine cell lineages of the intestine. Dev. Biol. 313, 58–66.
Farin, H.F., Van Es, J.H., Clevers, H., 2012. Redundant sources of Wnt regulate intestinal stem cells and promote formation of Paneth cells. Gastroenterology 143, 1518–1529 e1517.
Firth, S.M., Baxter, R.C., 2002. Cellular actions of the insulin-like growth factor binding proteins. Endocr. Rev. 23, 824–854.
Flasse, L.C., Stern, D.G., Pirson, J.L., Manfroid, I., Peers, B., Voz, M.L., 2013. The bHLH transcription factor Ascl1a is essential for the specification of the intestinal secretory cells and mediates Notch signaling in the zebrafish intestine. Dev. Biol. 376, 187–197.
Ganz, J., Kroehne, V., Freudenreich, D., Machate, A., Geffarth, M., Braasch, I., Kaslin, J., Brand, M., 2014. Subdivisions of the adult zebrafish pallium based on molecular marker analysis. F1000Research 3, 308.
Hao, H.X., Xie, Y., Zhang, Y., Charlat, O., Oster, E., Avello, M., Lei, H., Mickanin, C., Liu, D., Ruffner, H., Mao, X., Ma, Q., Zamponi, R., Bouwmeester, T., Finan, P.M., Kirschner, M.W., Porter, J.A., Serluca, F.C., Cong, F., 2012. ZNRF3 promotes Wnt receptor turnover in an R-spondin-sensitive manner. Nature 485, 195–200.
Haramis, A.P., Hurlstone, A., van der Velden, Y., Begthel, H., van den Born, M., Offerhaus, G.J., Clevers, H.C., 2006. Adenomatous polyposis coli-deficient zebrafish are susceptible to digestive tract neoplasia. EMBO Rep. 7, 444–449.
Hayakawa, Y., Sakitani, K., Konishi, M., Asfaha, S., Niikura, R., Tomita, H., Renz, B.W., Tailor, Y., Macchini, M., Middelhoff, M., Jiang, Z., Tanaka, T., Dubeykovskaya, Z.A., Kim, W., Chen, X., Urbanska, A.M., Nagar, K., Westphalen, C.B., Quante, M., Lin, C.S., Gershon, M.D., Hara, A., Zhao, C.M., Chen, D., Worthley, D.L., Koike, K., Wang, T.C., 2017. Nerve growth factor promotes gastric tumorigenesis through aberrant cholinergic signaling. Cancer Cell 31, 21–34.
He, T.C., Sparks, A.B., Rago, C., Hermeking, H., Zawel, L., da Costa, L.T., Morin, P.J., Vogelstein, B., Kinzler, K.W., 1998. Identification of c-MYC as a target of the APC pathway. Science New York, N.Y 281, 1509–1512.
Kim, T.H., Escudero, S., Shivdasani, R.A., 2012. Intact function of Lgr5 receptor-expressing intestinal stem cells in the absence of Paneth cells. Proc. Natl. Acad. Sci. U. S. A 109, 3932–3937.
Koo, B.K., Spit, M., Jordens, I., Low, T.Y., Stange, D.E., van de Wetering, M., van Es, J.H., Mohammed, S., Heck, A.J., Maurice, M.M., Clevers, H., 2012. Tumour suppressor RNF43 is a stem-cell E3 ligase that induces endocytosis of Wnt receptors. Nature 488, 665–669.
Korinek, V., Barker, N., Moerer, P., van Donselaar, E., Huls, G., Peters, P.J., Clevers, H., 1998. Depletion of epithelial stem-cell compartments in the small intestine of mice lacking Tcf-4. Nat. Genet. 19, 379–383.
Kuemmerle, J.F., 2012. Insulin-like growth factors in the gastrointestinal tract and liver. Endocrinol Metab. Clin. N. Am. 41, 409–423 (vii).
Li, J., Prochaska, M., Maney, L., Wallace, K.N., 2019. Development and organization of the zebrafish intestinal epithelial stem cell niche. Dev. Dynam.
Lickwar, C.R., Camp, J.G., Weiser, M., Cocchiaro, J.L., Kingsley, D.M., Furey, T.S., Sheikh, S.Z., Rawls, J.F., 2017. Genomic dissection of conserved transcriptional regulation in intestinal epithelial cells. PLoS Biol. 15, e2002054.
Lin, J., Wang, X., Dorsky, R.I., 2011. Progenitor expansion in apc mutants is mediated by Jak/Stat signaling. BMC Dev. Biol. 11, 73.
Lustig, B., Jerchow, B., Sachs, M., Weiler, S., Pietsch, T., Karsten, U., van de Wetering, M., Clevers, H., Schlag, P.M., Birchmeier, W., Behrens, J., 2002. Negative feedback loop of Wnt signaling through upregulation of conductin/axin2 in colorectal and liver tumors. Mol. Cell. Biol. 22, 1184–1193.
Martin, B.L., Kimelman, D., 2012. Canonical Wnt signaling dynamically controls multiple stem cell fate decisions during vertebrate body formation. Dev. Cell 22, 223–232.
McCurley, A.T., Callard, G.V., 2008. Characterization of housekeeping genes in zebrafish: male-female differences and effects of tissue type, developmental stage and chemical treatment. BMC Mol. Biol. 9, 102.
Muncan, V., Faro, A., Haramis, A.P., Hurlstone, A.F., Wienholds, E., van Es, J., Korving, J., Begthel, H., Zivkovic, D., Clevers, H., 2007. T-cell factor 4 (Tcf7l2) maintains proliferative compartments in zebrafish intestine. EMBO Rep. 8, 966–973.
Neal, J.T., Peterson, T.S., Kent, M.L., Guillemin, K., 2013. H. pylori virulence factor CagA increases intestinal cell proliferation by Wnt pathway activation in a transgenic zebrafish model. Dis. Model. Mech. 6, 802–810.
Ng, A.N., de Jong-Curtain, T.A., Mawdsley, D.J., White, S.J., Shin, J., Appel, B., Dong, P.D., Stainier, D.Y., Heath, J.K., 2005. Formation of the digestive system in zebrafish: III. Intestinal epithelium morphogenesis. Dev. Biol. 286, 114–135.
Noah, T.K., Donahue, B., Shroyer, N.F., 2011. Intestinal development and differentiation. Exp. Cell Res. 317, 2702–2710.
Olden, T., Akhtar, T., Beckman, S.A., Wallace, K.N., 2008. Differentiation of the zebrafish enteric nervous system and intestinal smooth muscle. Genesis 46, 484–498.
Pilon, N., Oh, K., Sylvestre, J.R., Savory, J.G., Lohnes, D., 2007. Wnt signaling is a key mediator of Cdx1 expression in vivo. Development 134, 2315–2323.

Pogoda, H.M., von der Hardt, S., Herzog, W., Kramer, C., Schwarz, H., Hammerschmidt, M., 2006. The proneural gene ascl1a is required for endocrine differentiation and cell survival in the zebrafish adenohypophysis. Development 133, 1079–1089. Cambridge, England.

Roach, G., Heath Wallace, R., Cameron, A., Emrah Ozel, R., Hongay, C.F., Baral, R., Andreescu, S., Wallace, K.N., 2013. Loss of ascl1a prevents secretory cell differentiation within the zebrafish intestinal epithelium resulting in a loss of distal intestinal motility. Dev. Biol. 376, 171–186.

Sato, A., 2007. Tuft cells. Anat. Sci. Int. 82, 187–199.

Sato, T., van Es, J.H., Snippert, H.J., Stange, D.E., Vries, R.G., van den Born, M., Barker, N., Shroyer, N.F., van de Wetering, M., Clevers, H., 2011. Paneth cells constitute the niche for Lgr5 stem cells in intestinal crypts. Nature 469, 415–418.

Schall, K.A., Holoyda, K.A., Grant, C.N., Levin, D.E., Torres, E.R., Maxwell, A., Pollack, H.A., Moats, R.A., Frey, M.R., Darehzereshki, A., Al Alam, D., Lien, C., Grikscheit, T.C., 2015. Adult zebrafish intestine resection: a novel model of short bowel syndrome, adaptation, and intestinal stem cell regeneration. Am. J. Physiol. Gastrointest. Liver Physiol. 309, G135–G145.

Schutz, B., Jurastow, I., Bader, S., Ringer, C., von Engelhardt, J., Chubanov, V., Gudermann, T., Diener, M., Kummer, W., Krasteva-Christ, G., Weihe, E., 2015. Chemical coding and chemosensory properties of cholinergic brush cells in the mouse gastrointestinal and biliary tract. Front. Physiol. 6, 87.

Shoubridge, C.A., Steeb, C.B., Read, L.C., 2001. IGFBP mRNA expression in small intestine of rat during postnatal development. Am. J. Physiol. Gastrointest. Liver Physiol. 281, G1378–G1384.

Shyer, A.E., Huycke, T.R., Lee, C., Mahadevan, L., Tabin, C.J., 2015. Bending gradients: how the intestinal stem cell gets its home. Cell 161, 569–580.

Shyer, A.E., Tallinen, T., Nerurkar, N.L., Wei, Z., Gil, E.S., Kaplan, D.L., Tabin, C.J., Mahadevan, L., 2013. Villification: how the gut gets its villi. Science 342, 212–218. New York, N.Y.

Sun, D., Zhang, Y., Wang, C., Hua, X., Zhang, X.A., Yan, J., 2013. Sox9-related signaling controls zebrafish juvenile ovary-testis transformation. Cell Death Dis. 4, e930.

Tetsu, O., McCormick, F., 1999. Beta-catenin regulates expression of cyclin D1 in colon carcinoma cells. Nature 398, 422–426.

Tian, A., Benchabane, H., Wang, Z., Zimmerman, C., Xin, N., Perochon, J., Kalna, G., Sansom, O.J., Cheng, C., Cordero, J.B., Ahmed, Y., 2017. Intestinal stem cell overproliferation resulting from inactivation of the APC tumor suppressor requires the transcription cofactors Earthbound and Erect wing. PLoS Genet. 13, e1006870.

Troll, J.V., Hamilton, M.K., Abel, M.L., Ganz, J., Bates, J.M., Stephens, W.Z., Melancon, E., van der Vaart, M., Meijer, A.H., Distel, M., Eisen, J.S., Guillemin, K., 2018. Microbiota promote secretory cell determination in the intestinal epithelium by modulating host Notch signaling. Development 145. Cambridge, England.

Van Landeghem, L., Santoro, M.A., Mah, A.T., Krebs, A.E., Dehmer, J.J., McNaughton, K.K., Helmrath, M.A., Magness, S.T., Lund, P.K., 2015. IGF1 stimulates crypt expansion via differential activation of 2 intestinal stem cell populations. FASEB J. Off. Publ. Fed. Am. Soc. Exp. Biol. 29, 2828–2842.

Wallace, K.N., Akhter, S., Smith, E.M., Lorent, K., Pack, M., 2005a. Intestinal growth and differentiation in zebrafish. Mech. Dev. 122, 157–173.

Wallace, K.N., Akhter, S., Smith, E.M., Lorent, K., Pack, M., 2005b. Intestinal growth and differentiation in zebrafish. Mech. Dev. 122, 157–173.

Wallace, K.N., Pack, M., 2003. Unique and conserved aspects of gut development in zebrafish. Dev. Biol. 255, 12–29.

Wang, Q., Tan, X., Jiao, S., You, F., Zhang, P.J., 2014. Analyzing cold tolerance mechanism in transgenic zebrafish (Danio rerio). PLoS One 9, e102492.

Wang, Y., Rovira, M., Yusuff, S., Parsons, M.J., 2011. Genetic inducible fate mapping in larval zebrafish reveals origins of adult insulin-producing beta-cells. Development 138, 609–617. Cambridge, England.

Wang, Y.C., Gallego-Arteche, E., Iezza, G., Yuan, X., Matli, M.R., Choo, S.P., Zuraek, M.B., Gogia, R., Lynn, F.C., German, M.S., Bergsland, E.K., Donner, D.B., Warren, R.S., Nakakura, E.K., 2009. Homeodomain transcription factor NKX2.2 functions in immature cells to control enteroendocrine differentiation and is expressed in gastrointestinal neuroendocrine tumors. Endocr. Relat. Cancer 16, 267–279.

Westerfield, M., 1993. The Zebrafish Book : a Guide for the Laboratory Use of Zebrafish (Brachydanio Rerio). M. Westerfield, Eugene, OR.

Westphalen, C.B., Asfaha, S., Hayakawa, Y., Takemoto, Y., Lukin, D.J., Nuber, A.H., Brandtner, A., Setlik, W., Remotti, H., Muley, A., Chen, X., May, R., Houchen, C.W., Fox, J.G., Gershon, M.D., Quante, M., Wang, T.C., 2014. Long-lived intestinal tuft cells serve as colon cancer-initiating cells. J. Clin. Investig. 124, 1283–1295.

Winesett, D.E., Ulshen, M.H., Hoyt, E.C., Mohapatra, N.K., Fuller, C.R., Lund, P.K., 1995. Regulation and localization of the insulin-like growth factor system in small bowel during altered nutrient status. Am. J. Physiol. 268, G631–G640.

Wohrle, S., Wallmen, B., Hecht, A., 2007. Differential control of Wnt target genes involves epigenetic mechanisms and selective promoter occupancy by T-cell factors. Mol. Cell. Biol. 27, 8164–8177.

Wong, V.W., Stange, D.E., Page, M.E., Buczacki, S., Wabik, A., Itami, S., van de Wetering, M., Poulsom, R., Wright, N.A., Trotter, M.W., Watt, F.M., Winton, D.J., Clevers, H., Jensen, K.B., 2012. Lrig1 controls intestinal stem-cell homeostasis by negative regulation of ErbB signalling. Nat. Cell Biol. 14, 401–408.

Xie, Y., Zamponi, R., Charlat, O., Ramones, M., Swalley, S., Jiang, X., Rivera, D., Tschantz, W., Lu, B., Quinn, L., Dimitri, C., Parker, J., Jeffery, D., Wilcox, S.K., Watrobka, M., LeMotte, P., Granda, B., Porter, J.A., Myer, V.E., Loew, A., Cong, F., 2013. Interaction with both ZNRF3 and LGR4 is required for the signalling activity of R-spondin. EMBO Rep. 14, 1120–1126.

Yan, D., Wiesmann, M., Rohan, M., Chan, V., Jefferson, A.B., Guo, L., Sakamoto, D., Caothien, R.H., Fuller, J.H., Reinhard, C., Garcia, P.D., Randazzo, F.M., Escobedo, J., Fantl, W.J., Williams, L.T., 2001. Elevated expression of axin2 and hnkd mRNA provides evidence that Wnt/beta -catenin signaling is activated in human colon tumors. Proc. Natl. Acad. Sci. U. S. A 98, 14973–14978.

Yanai, H., Atsumi, N., Tanaka, T., Nakamura, N., Komai, Y., Omachi, T., Tanaka, K., Ishigaki, K., Saiga, K., Ohsugi, H., Tokuyama, Y., Imahashi, Y., Ohe, S., Hisha, H., Yoshida, N., Kumano, K., Kon, M., Ueno, H., 2017. Intestinal stem cells contribute to the maturation of the neonatal small intestine and colon independently of digestive activity. Sci. Rep. 7, 9891.

Zhao, C.M., Hayakawa, Y., Kodama, Y., Muthupalani, S., Westphalen, C.B., Andersen, G.T., Flatberg, A., Johannessen, H., Friedman, R.A., Renz, B.W., Sandvik, A.K., Beisvag, V., Tomita, H., Hara, A., Quante, M., Li, Z., Gershon, M.D., Kaneko, K., Fox, J.G., Wang, T.C., Chen, D., 2014. Denervation suppresses gastric tumorigenesis. Sci. Transl. Med. 6, 250ra115.